Ore Geology Reviews 105 (2019) 273–294

Contents lists available at ScienceDirect

Ore Geology Reviews

journal homepage: www.elsevier.com/locate/oregeorev

New insights into the geology and tectonics of the San Dimas mining district, Sierra Madre Occidental, Mexico

Paula Montoya-Lopera[a], Luca Ferrari[a,*], Gilles Levresse[a], Fanis Abdullin[b], Luis Mata[c]

[a] Centro de Geociencias, Universidad Nacional Autónoma de México, Campus Juriquilla, 76230 Querétaro, Qro., Mexico
[b] CONACyT–Centro de Geociencias, Universidad Nacional Autónoma de México, Campus Juriquilla, 76230 Querétaro, Qro., Mexico
[c] First Majestic Silver Corp., Tayoltita, Dgo., Mexico

ARTICLE INFO

Keywords:
Sierra Madre Occidental
San Dimas mining district
Epithermal deposit
Geochronology
Volcanic stratigraphy

ABSTRACT

The San Dimas district is a world-class silver-gold low-sulfidation epithermal deposit located in the central part of the Sierra Madre Occidental of Mexico, within the eastern part of the Gulf of California extensional province. Previous works assumed a single period of mineralization between ~38.5 and 31.9 Ma, which is at odds with the existence of vein systems with two different orientations and Ag/Au ratios. We present a re-evaluation of this district based on new zircon U/Pb and apatite fission-track ages as well as petrographic and field observations of mineralization styles. Our study also includes two new prospective areas of Causita and Mala Noche located to the south of the main district.

Within the Lower Volcanic Complex, we identify a Late Cretaceous volcanic succession (~77 to 69 Ma) correlative with the Tarahumara formation from southern Sonora and coeval with the San Ignacio batholith exposed to the west. This volcanic succession hosts Au-rich mineralized sub-volcanic felsic bodies yielding slightly younger ages and is covered by Paleocene intermediate lavas with hypabyssal intrusions with ages around 48 Ma. A voluminous intrusive suite (Piaxtla batholith and associated dike swarms) was emplaced in the region between ~49 and 44 Ma. Early extensional basins were filled by a continental sedimentary sequence (Palmas formation), which yielded U/Pb age peaks at 66 and 56 Ma from detrital zircons and a maximum depositional age of ~43 Ma. The last magmatic activity, as in the rest of the Sierra Madre Occidental, consists of silicic ignimbrites and less basaltic lava flows clustered in two pulses of ~31.5–29 Ma and 24–20 Ma.

NNW–SSE extensional fault systems expose the mineralization and tilted all the succession prior to the emplacement of a ~24 Ma ignimbrite package. This late Oligocene extension, associated to the early stage of the Gulf of California rift, is confirmed by apatite fission-track dating of samples from the Piaxtla batholith, which consistently indicate an episode of cooling at 25–23 Ma followed by a second episode at ~12.5 Ma. Our absolute ages and geologic mapping allow to infer that an older, WSW–ENE trending normal fault system with up to 1 km of displacement must exist between the San Dimas district and the Causita area to the south. This fault system, currently buried beneath Oligocene–Miocene ignimbrites, may have controlled the intrusion of the Piaxtla batholith and played a crucial role in the preservation of large vein systems of San Dimas in a tectonic depression setting.

The main epithermal mineralization is associated with two kinds of structures: Ag/Au veins with WSW–ENE to E–W orientation and Au/Ag veins with NNW–SSE to N–S orientation. The dominant Ag/Au veins slightly postdate the Piaxtla intrusive suite and partly recycled older felsic intrusion with porphyry mineralization. The NNW–SSE to N–S Au/Ag veins are most probably associated with the Oligocene silicic volcanism.

1. Introduction

A proper understanding of the formation and preservation of mineral deposits in continental settings implies assessing the dynamic interaction among magmatic, tectonic, erosional, and depositional processes. This approach is particularly important in the case of western Mexico, which has undergone a complex tectono-magmatic history since the Cretaceous (Ferrari et al., 2017). In this region, the Sierra Madre Occidental (SMO) geologic province hosts numerous important porphyry and epithermal deposits mostly occurring in its western side,

* Corresponding author.
E-mail address: luca@unam.mx (L. Ferrari).

https://doi.org/10.1016/j.oregeorev.2018.12.020
Received 13 August 2018; Received in revised form 4 December 2018; Accepted 28 December 2018
Available online 02 January 2019
0169-1368/

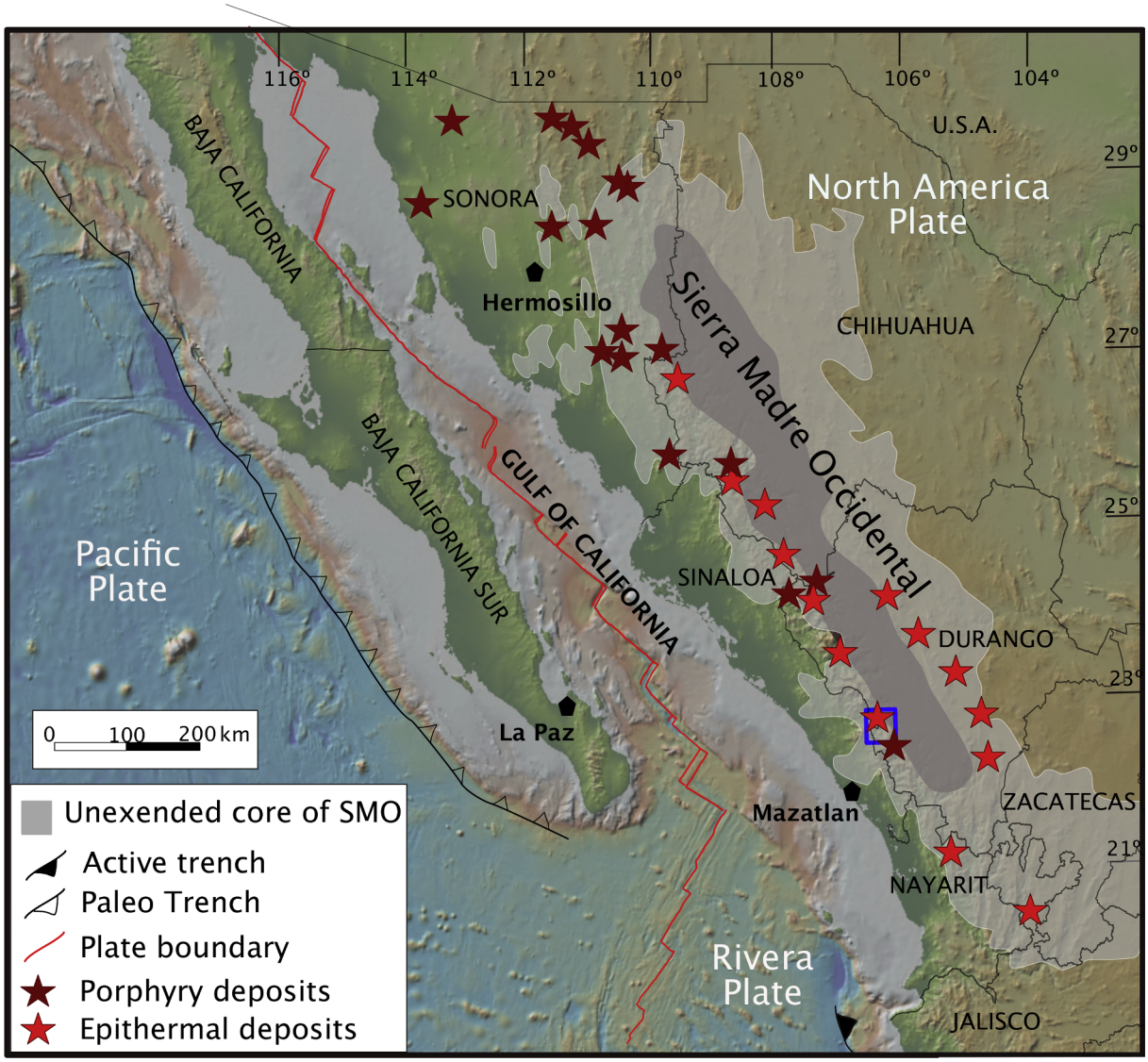

Fig. 1. Geodynamic context of western Mexico and main porphyry and epithermal deposits of the Sierra Madre Occidental volcanic province. The blue rectangle represents the study area. (For interpretation of the references to color in this figure legend, the reader is referred to the web version of this article.)

a portion that represents the eastern rifted margin of the Gulf of California (Fig. 1). Several reviews and classifications of the SMO mineralization have been proposed in past decades. The initial attempts relied on the concept of metallogenic provinces or belts, where mineralization is essentially tied to a geographic domain and produced by the interaction of arc magmatism with a certain type of basement terrane (e.g. Damon et al., 1981, 1983; Campa and Coney, 1983; Salas, 1994). More recent reviews (e.g. Staude and Barton, 2001; Camprubí, 2013; Camprubí and Albinson, 2007) placed each mineralization type into a specific magmatic-tectonic episode since Mesozoic, implicitly recognizing the dynamic nature of this plate margin and the possibility of superposition of mineralization events. Several studies have also been devoted to classifying the SMO epithermal deposits based on fluid geochemistry and physical parameters (e.g. Smith et al., 1982; Clarke and Titley, 1988; Albinson et al., 2001; Camprubí and Albinson, 2007). However, reviews and analytical studies are significantly limited by the fact that most parts of the SMO lack a good geochronologic control and a detailed geologic description of veins systems, which may jeopardize a correct interpretation of a mineral deposit development.

The San Dimas mining district, centered at the town of Tayoltita, is a world-class silver-gold epithermal deposit and possibly the archetype of such deposits in the SMO (Locke, 1918; Davidson, 1932; Henshaw, 1953; Clarke, 1986). Mined since the 18th century, the San Dimas district contains more than 200 discovered Ag-Au veins, located in five blocks separated by major NNW-striking normal faults. Despite being a world reference for low-sulfidation Ag-Au epithermal veins, the mineralization model for San Dimas has not been improved significantly since the middle of the past century. The current stratigraphic overview is based on field and mine observations, supported by petrographic and geochronologic studies (Nemeth, 1976; Henry and Fredrikson, 1987; Enriquez and Rivera, 2001a,b; Henry et al., 2003). The rocks hosting the mineralization are not dated and the Ag-Au veins have been traditionally considered to be developed in a single mineralization episode between ~41 and ~31 Ma (Enríquez and Rivera, 2001b; Enriquez et al., 2018). However, most these ages, obtained by the K–Ar method, are not always reliable given the widespread hydrothermal alteration of the district. The difference in vein orientation with variable Ag/Au ratio through the district are also at odd with the idea of a single mineralization episode.

In this study, we present a revision of the geology and stratigraphy of the San Dimas district as well as of adjacent areas based on fieldwork at surface and in mine interior, supported by a detailed petrographic study and U/Pb and apatite fission-track ages of the whole geologic column. This provides a robust geologic and geochronologic context

towards a better understanding of the mineralization events that will be described in detail in a forthcoming paper (Montoya-Lopera et al., submitted for publication).

2. Previous studies

2.1. Regional geology and tectonic setting

As a physiographic province, the SMO comprises a high plateau with an average elevation exceeding 2000 m above sea level that cover an area ~1200 km long and ~200 to 400 km wide extending from the Mexico–US border approximately to Latitude 21° N, where it intersects the Trans Mexican Volcanic Belt (Fig. 1). The western part of the SMO high plateau is cut by normal faults systems that are part of the Gulf of California rift and where most ore deposits are exposed. As an igneous province, the SMO includes Late Cretaceous to early Miocene rocks formed during two main periods of continental magmatic activity (McDowell and Keizer, 1977; Ferrari et al., 2017). The first period, concurrent with the Laramide orogeny, produced a dominantly intermediate intrusive suite and its volcanic counterpart, associated with a normal supra-subduction magmatic arc active between ~100 and 50 Ma (Gastil, 1975; McDowell et al., 2001; Henry et al., 2003; Ortega-Gutiérrez et al., 2014). These rocks, traditionally named Lover Volcanic Complex (LVC) (McDowell and Keizer, 1977), formed the Sonora, Sinaloa, and the Jalisco batholiths, as well as the Late Cretaceous to Paleocene volcanic succession of the Tarahumara Formation in Sonora (Wilson and Rocha, 1949; McDowell et al., 2001), and equivalent rocks in the Jalisco Block (Ferrari and Rosas-Elguera, 2000; Valencia et al., 2013) (Fig. 1). Volcanic successions of this age have been inferred in Sinaloa and Durango, but no radiometric ages have been provided so far.

After a transitional period that lasted until the late Eocene (Ferrari et al., 2017), volcanism became dominated by rhyolitic ignimbrites with less basaltic lavas, building one of the largest silicic volcanic provinces on Earth (Bryan and Ferrari, 2013). Defined as the Upper Volcanic Supergroup (UVS) (McDowell and Keizer, 1977), these rocks were emplaced mostly in two episodes of ignimbrite flare up at ~35 to 29 Ma along the entire province and at ~24 to 20 Ma in its southern part (Ferrari et al., 2002, 2007; McDowell and McIntosh, 2012). Mafic lavas with both asthenosphere and mantle lithosphere affinity are found interspersed within the ignimbrite successions, often associated with normal faulting (Ferrari et al., 2017). Extensional basins and associated continental sedimentary deposits formed between ~27 and ~15 Ma in a NNW-trending belt along the western half of the SMO, spanning the western part of Sonora (McDowell et al., 1997; Nourse et al., 1994; Gans, 1997; González León et al., 2000; Wong et al., 2010; Murray et al., 2013) and most of Sinaloa and Nayarit (Ferrari et al., 2013) (Fig. 1). The temporal and spatial association of the silicic (or felsic) to bimodal magmatism of the UVS with crustal extension supports the idea that these processes represent the beginning of the rifting process that led to the formation of the Gulf of California (Bryan and Ferrari, 2013; Ferrari et al., 2013, 2017).

The San Dimas mining district lies within the central part of the SMO, near the Sinaloa–Durango state border (Fig. 1). The geology of this part of the SMO is summarized in Fig. 2 and is briefly described in the following based on recent regional works presented in Ferrari et al. (2013, 2017). The basement predating the continental batholiths is exposed in the western part of the region in the state of Sinaloa and consists of strongly folded metasedimentary and meta-volcanic rocks, deformed granitoids, phyllite sandstones, quartzites, and quartz-biotite-muscovite schists with ages spanning from Jurassic to Early Cretaceous (Henry and Fredrikson, 1987; Henry et al., 2003). These rocks are locally covered by Albian–Cenomanian limestones north of Mazatlán (Bonneau, 1970). The LVC consists of granite, granodiorite and diorite intrusive rocks exposed in the coastal areas and along the lower course of the main rivers, with ages progressively younger to the east. They form two main plutonic complexes: the San Ignacio batholith exposed towards the coast with mostly Late Cretaceous to early Paleocene ages; and, the Piaxtla batholith, cropping out towards the east along the Piaxtla and Presidio rivers with mostly Eocene ages (Fig. 2). The plutonic rocks were extensively studied by Henry (1975), Henry et al. (2003), who published many K–Ar and four U/Pb ages. Volcanic rocks consisting dominantly of ignimbrites with less lava flows are intruded by the Piaxtla batholith. Andesite lava flows cover these successions and the San Ignacio batholith and are sometimes intruded by the Eocene plutonic rocks. None of these volcanic successions have been dated so far.

Continental conglomerates and sandstones fill intermontane basins and separate the LVC from the UVS. The latter consists of two successions of silicic ignimbrites with minor basaltic lavas and some rhyolitic domes that covers the eastern part of the region. The first ignimbrite succession, mostly exposed towards the east in the Durango state, has been dated at ~32 to 30 Ma (McDowell and Keizer, 1977; McDowell and McIntosh, 2012; Ferrari et al., 2013). The second ignimbrite package, defined as the El Salto-Espinazo del Diablo succession by McDowell and Keizer (1977), yielded Ar–Ar ages of 24–23.5 Ma (McDowell and McIntosh, 2012) and is only exposed in the western part of the region. A NNW-trending extensional fault system, named Pueblo Nuevo–Tayoltita (Ferrari et al., 2013), separates the undeformed plateau of the SMO to the east, mostly in the Durango state, from the faulted and highly incised terrain to the west, in the Sinaloa state (Fig. 2). In this 90-km-wide, coast-parallel, extensional belt the El Salto-Espinazo del Diablo ignimbrite succession filled pre-existing valleys and lies in angular unconformity (20–30°) over the ~32 to 30 Ma ignimbrite successions, which indicate that a first extensional phase of deformation took place in the late Oligocene (Ferrari et al., 2013). Large volume rhyolitic domes with ages of ~29 to 28 Ma are aligned along the Pueblo Nuevo–Tayoltita fault system (Fig. 2). This coast-parallel extensional belt is characterized by several late Oligocene to middle Miocene graben, filled with conglomerates and some rhyolitic domes and basaltic lava flows (Ferrari et al., 2013).

2.2. Local geology

Previous knowledge on the geology and geochronology of the San Dimas district is summarized in the following. The LVC has been traditionally divided into informal geologic units primarily based on field observations. From base to top, these are the “Socavón rhyolite”, the “Buelna andesite”, and the “Portal rhyolite”, defined as a sequence of interlayered tuffs and lesser lava flows of felsic to intermediate composition (Locke, 1918; Davidson, 1932; Henshaw, 1953). These rocks are overlain unconformably by a succession of andesitic lavas named “Productive andesite” which is intruded by intermediate rocks called the “Arana intrusive andesite” and the “Arana intrusive diorite” (Henshaw, 1953) as well as by a felsic suite consisting of the “Piaxtla Granite” (partly mapped as Candelero granodiorite in Henry et al., 2003) and “Santa Lucia”, “Bolaños”, and “Santa Rita” dikes. Enríquez and Rivera (2001b) reported K–Ar ages obtained in a commercial laboratory for these intrusions. The intermediate intrusions yielded feldspar K–Ar ages ranging from 39.9 ± 1 to 36.6 ± 1 Ma, which are likely the result of partial resetting given that these intrusions lie near the core of the mineralized area. Henry et al. (2003) obtained a U/Pb age of 47.8 ± 1.0 Ma and hornblende and biotite K–Ar ages for six samples of the intrusive suite along the Piaxtla valley ranging from 51.2 ± 1.6 to 43.9 ± 0.3 Ma. In the Tayoltita area, biotite concentrates yielded K–Ar ages of 45.9 ± 1.2 and 45.1 ± 1.1 Ma (Enríquez and Rivera, 2001b), and an Ar–Ar age of 46.3 ± 0.1 Ma (Enriquez et al., 2018).

The LVC is separated from the younger rocks by a major erosional unconformity, marked by the so called “Las Palmas” and “Camichin” units made of conglomerate and red beds (Davidson, 1932; Henshaw, 1953). The overlying UVS, consists of a voluminous package of

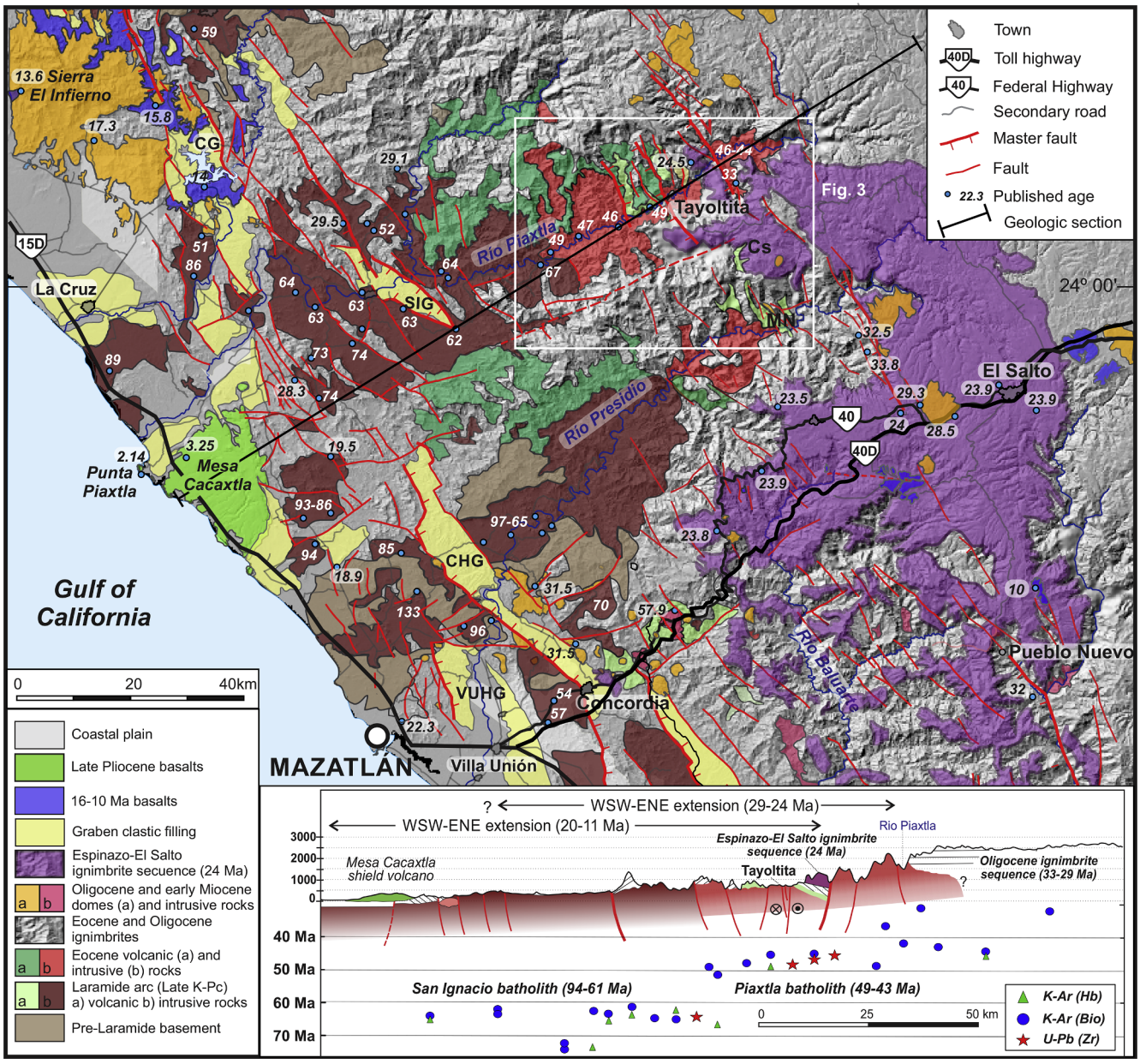

Fig. 2. Regional geologic map of central Sierra Madre Occidental showing the main extensional structures and published ages (modified from Henry and Fredrikson, 1987, and Ferrari et al., 2013). SIG—San Ignacio graben; CG—Conitaca graben; CHG – Concordia half-graben; VUHG – Villa Unión half-graben; MN—Mala Noche; Cs—Causita. The geologic section includes the ages of intrusive rocks in the Piaxtla valley (projected along the trace of the section) to show the sharp variation between the San Ignacio y Piaxtla batholiths.

ignimbrites, breccias, and less lava flows (Henshaw, 1953). Enríquez and Rivera (2001b) obtained a K–Ar age of 24.5 ± 0.9 Ma for the distinctive "Guarisamey andesite", located at the base of the sequence, and an age of 20.3 ± 0.8 Ma for the upper part of the ignimbrite succession.

The structural context has been addressed by Ballard (1980), who investigated the structural control of mineralization in the Tayoltita mine, and by Horner and Enriquez (1999), who studied the structural geology and tectonic control for the whole district. The most prominent structures are major north–northwest–trending normal faults with opposite vergence that divide the district into five blocks tilted to the ENE or WSW (Enriquez and Rivera, 2001a) (Fig. 3). All the major faults exhibit northeast–southwest extension, and dips that vary from nearly vertical to approximately 55° (Horner and Enriquez, 1999). E–W to WSW–ENE striking fractures, perpendicular to the major normal faults, are filled by quartz veins, dacite porphyry dikes, and pebble dikes, all cut by rhyolite porphyry dikes which occupy N–S to NNW–SSE trending fissures (Smith et al., 1982). Horner and Enriquez (1999) grouped the development of major faults, vein and dikes into three deformational events: 1) event D1, represented by tension gashes with E–W to ENE–WSW orientation with a slight right-lateral offset, developed in the late Eocene. These structures host the first hydrothermal vein systems. 2) Event D2, produced N–S-trending right-lateral strike-slip to transtensional faults due to a rotation of the maximum horizontal principal stress to a ~NE–SW position. In this stage, inferred to have occurred in the early Oligocene, a second set of hydrothermal veins developed. 3) Event D3 produced the major block faulting that affected the entire district along NNW–SSE-striking normal faults, which in some cases reactivated the former strike-slip faults during the late Oligocene–Miocene period. These faults hosted bimodal dikes, which are part of the UVS.

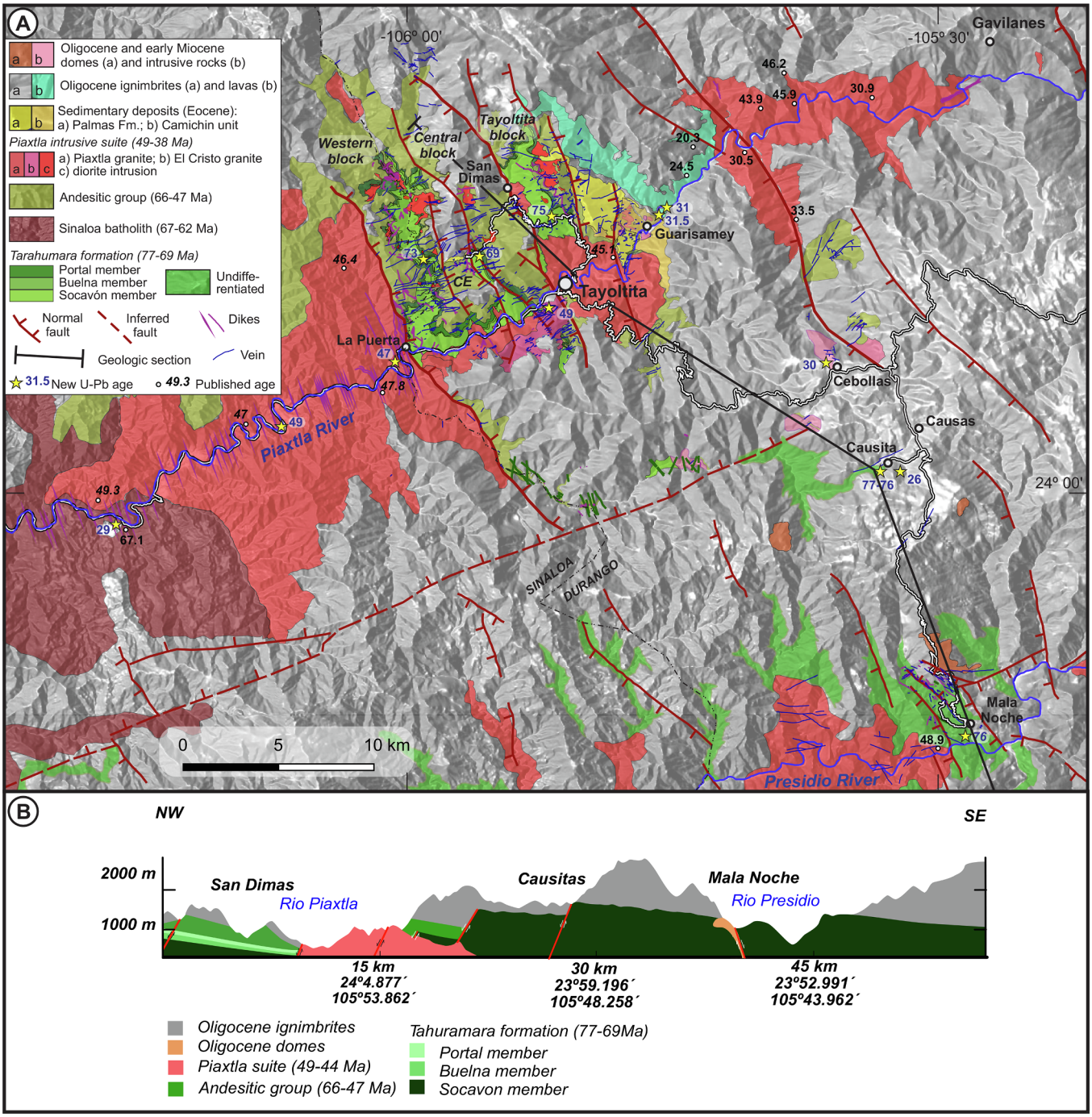

Fig. 3. A) Geologic map of San Dimas mining district and Causita-Mala Noche areas, with location of published and new ages. B) Geologic section.

3. Analytical techniques

3.1. Geologic mapping and sampling

A revision of the geologic cartography was carried out by detailed mapping (at a scale 1:10,000) along key transects along roadcuts that crossed all the geologic units of the district. Geologic observations were also made along the Piaxtla river and adjacent creeks. We also made observations along a transect to the south of the district up to the Presidio river valley to compare the stratigraphy of San Dimas with that of the Causita prospective area and the inactive Mala Noche mining area (Fig. 3). Based on the result of fieldwork and the revised stratigraphy we selected twenty-nine representative samples for petrographic and geochronological analyses. Some of these samples come from exploratory drillings provided by Primero Mining Corp (recently acquired by First Majestic Silver Corporation) that were chosen to obtain information from the lowermost part of the succession.

3.2. Petrography

Twenty-one thin-sections were analyzed petrographically. The petrographic study was made using an Olympus® BX-50 optical microscope with a Qimaging Micropublisher 5 Mp digital camera equipped with a Peltier-cooled CCD. Modal analyses were carried out using an average count of 600–800 points for igneous rocks. For rocks with porphyritic texture, phenocrysts modal proportions (crystal > 1 mm) are based on

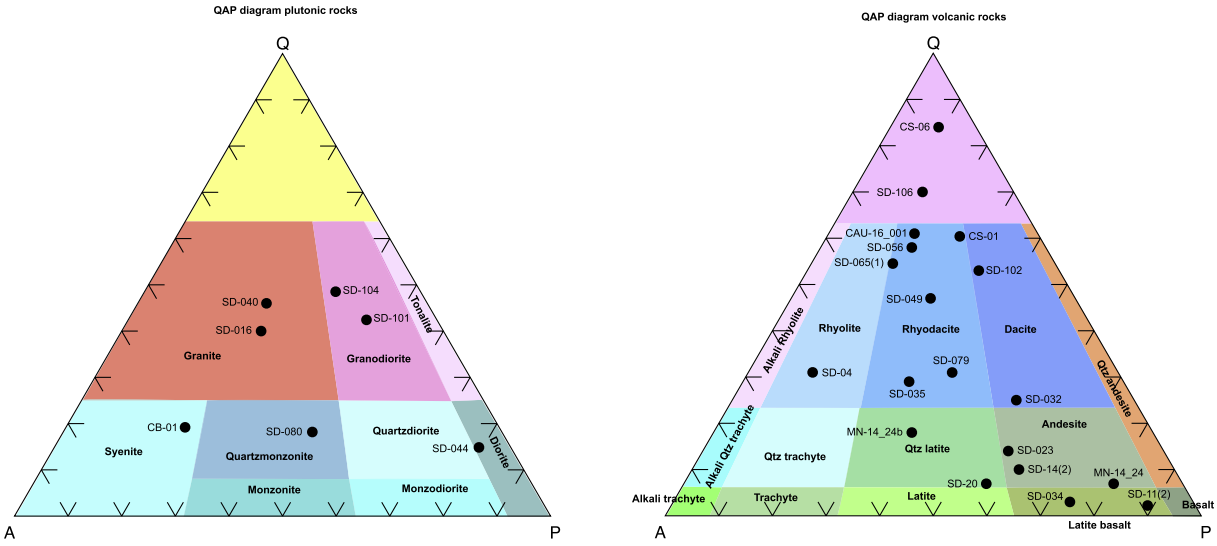

Fig. 4. Petrographic classification (Le Bas and Streckeisen, 1991) of studied samples.

a minimum of 800 points per thin-section. Samples were described according to the subcommission on the Systematic of Igneous Rocks standards (Le Maitre et al., 2002) and classified according to the Streckeisen QAP triangle for plutonic and volcanic rocks (Le Bas and Streckeisen, 1991) (Fig. 4). The composition of plagioclase was estimated by Michel-Levy's method wherever possible. Sedimentary rocks were classified according to the conventional FQR triangle for detritus samples (Folk, 1974).

3.3. U/Pb geochronology and zircon geochemistry

Twenty-nine rock samples with stratigraphic control were selected for U/Pb dating. The samples were crushed, powdered, and sieved (200–50 mesh). Heavy minerals were concentrated using conventional techniques. Zircon crystals were hand-picked under a binocular microscope and mounted with EpoFix® in a 2.5-cm-diameter plastic ring, and then, were polished. Laser ablation target points were selected based on cathodoluminescence images to identify zircon cores and overgrowth zones. Single-spot analyses were performed with a Resonetics RESOlution® LPX Pro (193 nm, ArF excimer) laser ablation system, coupled to a Thermo® Scientific iCAP® Qc quadrupole ICP-MS at Laboratorio de Estudios Isotópicos (LEI), at Centro de Geociencias, Campus Juriquilla, UNAM. For every zircon, each spot analysis consists in the acquisition of 15 s of background signal (gas blank), 30 s of ablation, and 15 s to allow the signal to reach the base-line again (washout). The spot diameter was of 33 μm, using a fluency of 6 J/cm^2 with a repetition rate of 5 Hz. Together with those isotopes required for the U/Pb age calculation (^{206}Pb, ^{207}Pb, ^{208}Pb, ^{232}Th, and ^{238}U), LA–ICP-MS permits to detect additional elements simultaneously such as major and trace elements and rare earth elements, etc. These compositional data may also be used to obtain information about the different magmatic pulses in term of mineral fertility. ICP-MS tuning follows the parameters reported in Solari et al. (2010) and Ortega-Obregón et al. (2014). Corrected isotope ratios and ages with errors were calculated with Iolite (Paton et al., 2011) using the VizualAge data reduction (Petrus and Kamber, 2012). Chemical compositions in zircons were obtained based on NIST standard glasses. "91500" zircon (Wiedenbeck et al., 1995) was used as a main reference mineral for zircon U/Pb analyses. For igneous samples, ~35 zircons were analyzed. The intrusive and volcanic ages are reported based on the weighted mean crystallization age into two standard deviations (Ludwig, 2008). Analyses outside of two standard deviation were discarded. Discordant percentages higher than twenty percent were not considered. For volcanic rocks, the preferred age was considered that of the youngest zircon populations. For igneous samples, crystals with noticeably old ages were interpreted as zircons inherited from the basement. For sedimentary samples, ~100 zircons were analyzed. The maximum age of sedimentation was associated to the younger zircons analyzed. The different family ages were reported using histograms and probability density diagrams.

3.4. Apatite fission-track thermochronology

Apatite fission-track (AFT) dating was performed at LEI Lab, using LA–ICP-MS-based technique (Hasebe et al., 2004; Donelick et al., 2005). Details of the methodology is described in Abdullin et al. (2018). In this experiment, Durango F-apatite, with an age of 31.4 ± 0.5 Ma (Hurford, 2019), was used for ζ-equivalent calibration (Hasebe et al., 2004; Donelick et al., 2005, Vermeesch, 2017) as well as for Cl measurements in unknown apatite samples (taking Durango as a primary standard, with 0.43 ± 0.03 wt% of Cl in Durango; Goldoff et al., 2012). Single-grain AFT ages with 1SE were calculated using IsoplotR (Vermeesch, 2017, 2018). The central (mean) AFT ages and different age peaks were obtained using RadialPlotter of Vermeesch (2009).

4. Results

4.1. Introduction

In this section we present our revision of the stratigraphy of the San Dimas mining district that integrates the results of new mapping and the petrographic and geochronologic studies. Table 1 presents the results obtained for twenty-nine representative samples of the stratigraphy of the San Dimas district and adjoining areas. Experimental results are presented in Figs. 5–8. For igneous rocks (Figs. 5, 6 and 8) we chose the mean age of the dominant population as the most reliable age, but Concordia diagrams are also presented to illustrate the quality of the data. Full analytical data are presented in Table 1a in the appendix. For sedimentary rocks we present probability density diagrams of detrital zircons (Fig. 7). AFT results are shown on Fig. 9 and Table 2a in the appendix. The petrographic characteristics of each geologic unit are presented in Table 2. Macro- and micro-photographs of the samples are presented in the appendix (Supplementary material, Figs. 1A–10A).

In our geological re-evaluation, the stratigraphic column is divided into five groups (Fig. 10): 1) the silicic to intermediate ignimbrites and lavas from the lower part of the LVC and the San Ignacio batholith; 2) the Andesitic Group, composed by intermediate lavas and hypabyssal intrusions; 3) the Piaxtla batholithic intrusion and associated dikes, 4)

Table 1
Summary of new U-Pb ages.

Sample	Geologic unit and location	Long. W (datum WGS84)	Lat. N (datum WGS84)	Elevation (m asl)	Rock type	Age (Ma)	Error (Ma)	Age type	Comments
Sierra Madre Occidental silicic large igneous province – Upper Volcanic Supergroup									
CS-06	Second flare-up. First ash flow above a conglomerate covering tilted ignimbrites at Causita	105°46′45.08″	24°0′47.72″	2595	Ash flow tuff	**26.2**	**0.29**	Tuffzirc average	MSWD = 0.77. Mean of 14 grains of the dominant population (max age)
SD-102	Silicic dike intruded by mafic dike, riverbed near La Puerta	106°00′23.57″	24°04′4.45″	415	Silicic pyroclastic dike	**27.0**	**1.00**	Tuffzirc average	MSWD = 0.16. Mean of 24 grains of the dominant population
SD-106	Silicic lava near riverbed. Road Tayoltita to San Ignacio	106°08′14.40″	23°59′31.23″	290	Porphyritic rhyolitic lava	**29.0**	**0.54**	Tuffzirc average	MSWD = 0.57. Mean of 26 grains of the dominant population
CB-01	Shallow intrusion just north of Cebollas, below ignimbrites	105°48′20.94″	24°4′246.02″	1200	Fine-grained, hb-rich syenite	**31.3**	**0.48**	Tuffzirc average	MSWD = 3.1. Mean of 14 grains of the dominant population
						30.0	0.76	Lower intercept	MSWD = 1.4
SD-034	Guarisamey andesite member right above SD 035. Piaxtla river east of Guarisamey	105°53′10.53″	24°08′21.87″	600	Porphyritic latite basaltic lava	**31.0**	**1.10**	Tuffzirc average	MSWD = 0.59. Mean of the 4 younger grains. Large xenocrystic population at ~43 to 45 Ma. Three Late Cretaceous xenocrysts.
SD-035	First volcanic unit above sedimentary unit. Piaxtla river east of Guarisamey	105°53′9.43″	24°08′13.25″	595	Reddish ignimbrites with plag, san, qz	**31.5**	**0.80**	Tuffzirc average	MSWD = 1.9. Mean of 6 the younger grains. Probable antecrystic population at ~32 Ma
Volcano-sedimentary unit									
SD-029	Camichin unit, road Tayoltita to Guarisamey	105°54′20.58″	24°07′19.07″	975	Lithic tuff	**43.2**	**2.30**	Max deposition age, mean of the 2 younger zircons.	One peak at 56 Ma. 20 zircons in the range 53–68 Ma, one at 140 Ma and two > 500 Ma
SD-031	Palmas Formation, road Tayoltita to Guarisamey	105°54′16.28″	24°07′26.96″	965	Lithic arkose	**52.1**	**1.40**	Max deposition age, mean of the 5 younger zircons.	Two peaks at 56 and 65 Ma. 99 Zircons in the range 52–82 Ma. One at 95 Ma.
Lower Volcanic Complex									
Piaxtla intrusive suite									
SD-023	"Santa Rita"-type dike cutting Piaxtla batholith, 3 km west of Tayoltita	105°56′50.26″	24°05′08.30″	543	Porphyritic andesite with plag, hb, bio and qz	**45.0**	**0.51**	Tuffzirc average	MSWD = 0.25. Mean of 24 grains of the dominant population
SD-032	"Bolaños"-type dike cutting Piaxtla batholith, road to Guarisamey, 3 km east of Tayoltita	105°54′08.25″	24°07′43.96″	790	Porphyritic dacite with qz, plag, hb	**45.4**	**0.66**	Tuffzirc average	MSWD = 0.41. Mean of 21 grains of the dominant population
SD-040	Piaxtla batholith, San Francisco tunnel	105°55′49.24″	24°06′36.25″	463	Fine grained granite with qz, plag, bio, hb, px	**45.2**	**0.85**	Tuffzirc average	MSWD = 1.5. Mean of 27 grains of the dominant population
SD-101	Piaxtla batholith, riverbed at La Puerta	106°00′29.15″	24°04′17.85″	417	White, coarse grained granodiorite with qz, plag, feld, hb, px, bio	**47.0**	**0.75**	Tuffzirc average	MSWD = 1.4. Mean of 29 grains of the dominant population
SD-079	Porphyritic andesite, "Santa Rita" dike, Santa Rita mine near entrance fo the main tunnel.	105°54′16.77″	24°07′11.02″	800	Porphyritic rhyodacite	**47.5**	**0.93**	Tuffzirc average	MSWD = 4.9. Mean of 27 grains of the dominant population
SD-065(1)	Porphyritic andesite, "Santa Lucia" dike, San Luis tunnel between Santa Lucia and San Salvador veins	105°58′21.58″	24°08′11.27″	799	Porphyritic rhyodacite	**48.0**	**0.67**	Tuffzirc average	MSWD = 1.4. Mean of 20 grains of the dominant population
SD-080	Porphyritic andesite, "Santa Lucia" dike, San Luis tunnel between Santa Lucia and San Salvador veins	105°58′21.58″	24°08′11.27″	799	Porphyritic quartzomonzonite	**48.0**	**0.46**	Tuffzirc average	MSWD = 1.3. Mean of 24 grains of the dominant population
SD-016	Piaxtla batholith, "El Cristo" facies, near entrance of the tunnel. Intrusive contact with Socavón member	105°56′15.30″	24°05′34.96″	573	Fine grained granite with qz, alk feld, plag, hb	**49.0**	**0.43**	Tuffzirc average	MSWD = 0.25. Mean of 35 grains of the dominant population. 9 xenocrysts in the range 74–65 Ma (age of Tarahumara Fm)

(*continued on next page*)

Table 1 (*continued*)

Sample	Geologic unit and location	Long. W (datum WGS84)	Lat. N (datum WGS84)	Elevation (m asl)	Rock type	Age (Ma)	Error (Ma)	Age type	Comments
SD-104	Piaxtla batholith, riverbed 7 km west of La Puerta	106°03′44.40″	24°02′20.50″	350	Medium to fine grained granodiorite with plag, qz, bio, hb	**49.1**	**0.94**	Tuffzirc average	MSWD = 0.94. Mean of 21 grains of the dominant population
San Ignacio batholith									
SD 107	San Ignacio batholith, 16 km east of San Ignacio. Locally completely altered to unconsolidated sand	106°16′9.50″	23°57′17.83″	253	Medium grained granodiorite	**64.2**	**0.90**	Tuffzirc average	MSWD = 3.2. Mean of 25 grains of the dominant population
Tarahumara formation									
SD-049	Portal member. San Jose tunnel, recess 598	105°59′53.92″	24°07′26.12″	878	Lithic rhyodacite ignimbrite	**69.0**	**1.70**	Tuffzirc average	MSWD = 0.92. Mean of 4 grains of the dominant population
SD-014(2)	Buelna member, 4 km SSW of San Dimas	105°58′15.89″	24°07′05.51″	665	Porphyritic andesitic lava	**69.0**	**0.85**	Tuffzirc average	MSWD = 3.6. Mean of 16 grains of the dominant population
SD-056	Porphyry intrusion within the Socavón member, stream at the Sinaloa-Durango border	105°59′50.07″	24°06′51.79″	620	Porphyry rhyodacite	**73.0**	**1.50**	Tuffzirc average	MSWD = 1.7. Mean of 14 grains of the dominant population
SD-004	Socavón member, Tayoltita to San Dimas road	105°55′49.12″	24°08′08.39″	1176	Lithic porphyritic rhyolitic lava	**75.0**	**0.77**	Tuffzirc average	MSWD = 1.02. Mean of 19 grains of the dominant population
SD-020	Socavón member, near Piaxtla river 2 km west of Tayoltita	105°56′49.18″	24°05′23.49″	570	Quartz latite lava	**75.4**	**0.80**	Tuffzirc average	MSWD = 0.57. Mean of 20 grains of the dominant population
MN-14_24b	Mala Noche drillhole. This rock is observed intruding the whole drilling	105°44′47.981″	23°54′15.923″	1038	Px-rich porphyritic quartz latite	**75.5**	**1.00**	Lower intercept	MSWD = 4.7
MN-14_24	Mala Noche drillhole.	105°44′47.95″	23°54′15.906″	950	Andesitic lava	**76.1**	**0.63**	Tuffzirc average	MSWD = 4.6. Mean of 28 grains of the dominant population
CAU-16_001	Causitas drillhole. This rock includes clast of the whole sequence. Dated as detrital	105°4656.21″	24°058.24	2358	Lithic rhyodacite lava	**76.5**		Peak in PDD	91 zircones in the range 70–83 Ma, one at 91 Ma and one at 131 Ma
CS-01	Lava hosting the an epithermal vein at Causita.	105°46′58.50″	24° 0′59.08″	2518	Rhyodacite ignimbrite	77.5		Peak in probability density diagram	93 zircons in the range 71–84 Ma, one at 90.5 Ma and four at 132–139 Ma
						77.7	**0.88**	Tuffzirc average	MSWD = 5.3. Mean of 31 grains of the dominant population

Preferred ages in bold.

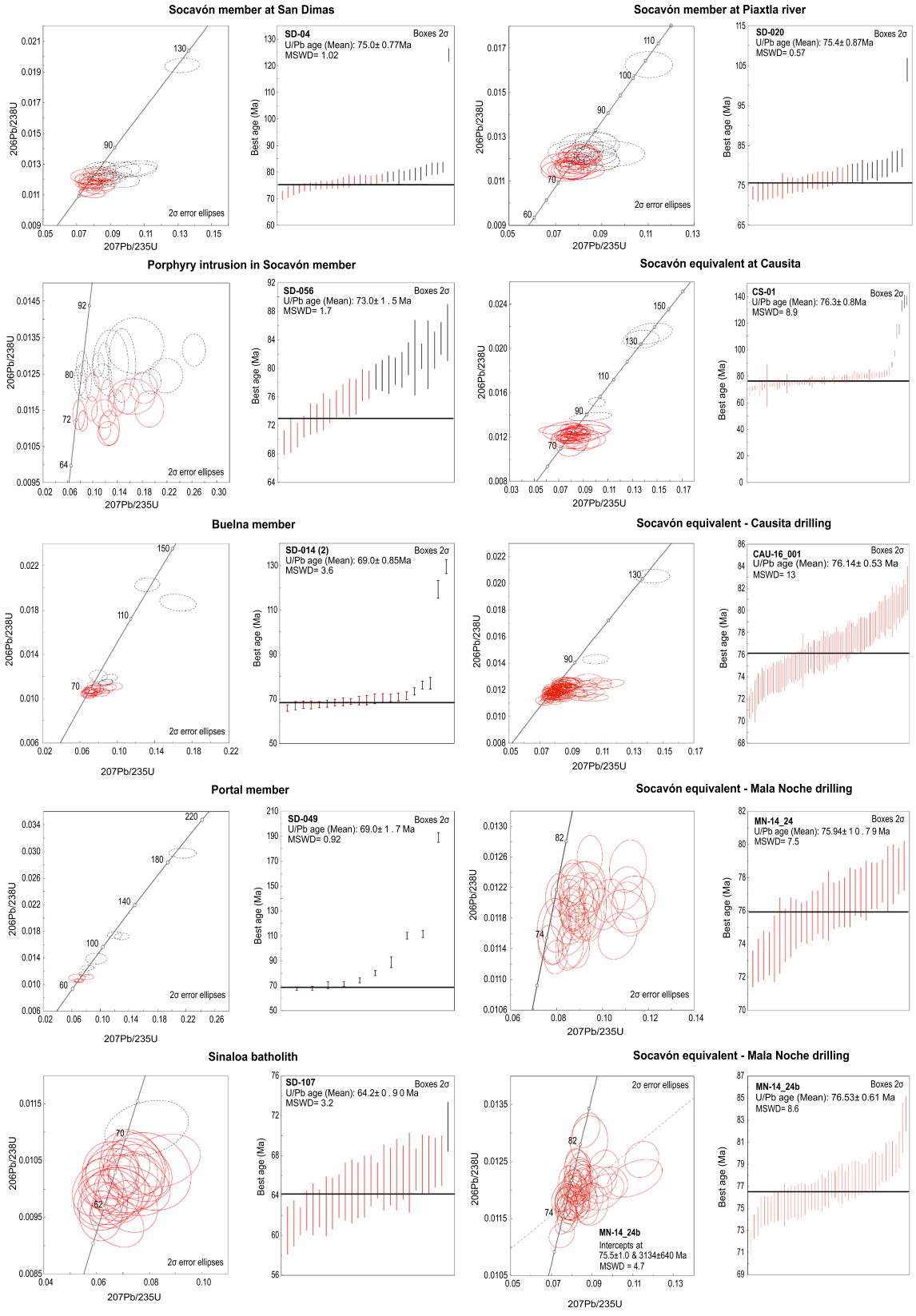

Fig. 5. Histograms and concordia diagrams of U-Pb ages for zircons of the Lower Volcanic Complex. Errors in calculated ages are 2σ. Black ellipses are data points not used in calculating the weighted mean.

the Las Palmas and Camichín continental sedimentary deposits, and 5) the Oligocene to early Miocene silicic ignimbrites, rhyolite domes and mafic lavas belonging to the UVS.

It is important to note that a large part of the district was affected by hydrothermal alteration, mainly in the form of propylitization (chlorite–epidote–calcite–pyrite). This alteration is pervasive at a local scale,

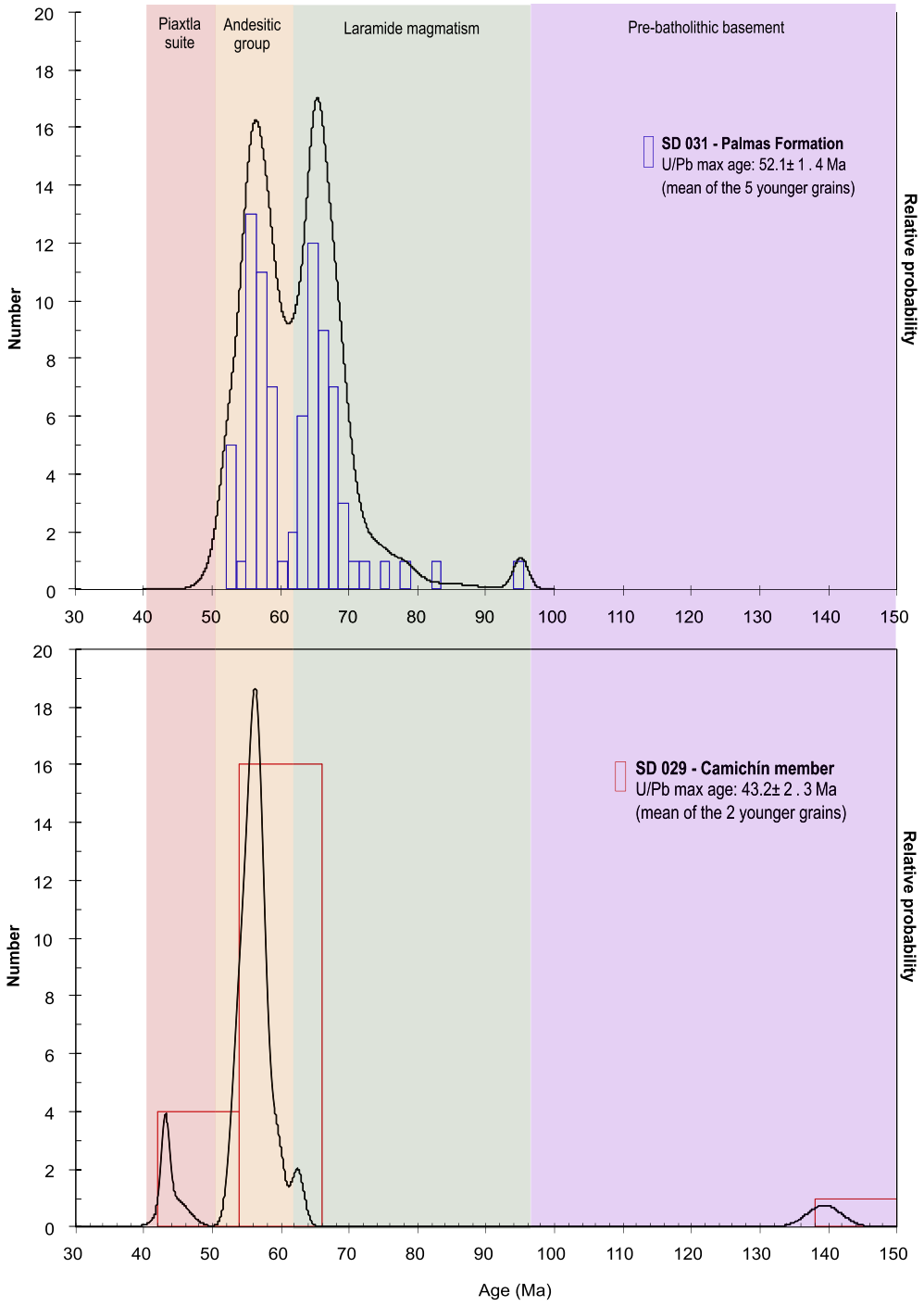

Fig. 6. Histograms and concordia diagrams of U-Pb ages for zircons of the Piaxtla intrusive suite. Errors in calculated ages are 2σ. Black ellipses are data points not used in calculating the weighted mean.

increases in intensity close to the mineralized structures and it is overprinted by phyllic alteration close to vein structures.

4.2. Lower volcanic complex

4.2.1. Late Cretaceous volcanic sequence

The oldest rocks belong to a thick volcanic succession exposed in the lower part of the valleys north of the Piaxtla River with a total thickness of approximately 2 km. The succession is composed by a series of andesitic to rhyolitic lava flows, tuffs, and breccias defined as the Socavón, Buelna and Portal members. The Socavón member consists of an alternating suite of rhyolitic and andesite lavas locally intruded by mineralized felsic porphyritic bodies. It commonly presents a porphyritic texture, reddish to gray in color, and consists of quartz > orthoclase > plagioclase > pyroxene > biotite and hornblende in a groundmass of fine plagioclase and glass with lithic fragments at the base. This member crops out throughout the district with up to 800 m of thickness. The alteration of mineralized porphyritic bodies is associated with pervasive secondary biotite overprinted by sodic–calcic (albite–actinolite–epidote) alteration around sinuous quartz, pyrite, and chalcopyrite veins. The mineralized bodies are exposed in the western Block in the Contraestaca area (Fig. 3). We obtained two ages of 75.4 ± 0.8 and 75.0 ± 0.7 Ma for the Socavón member (SD 020 and 004) and an age of 73.0 ± 1.5 Ma for a porphyry dacitic intrusion (SD

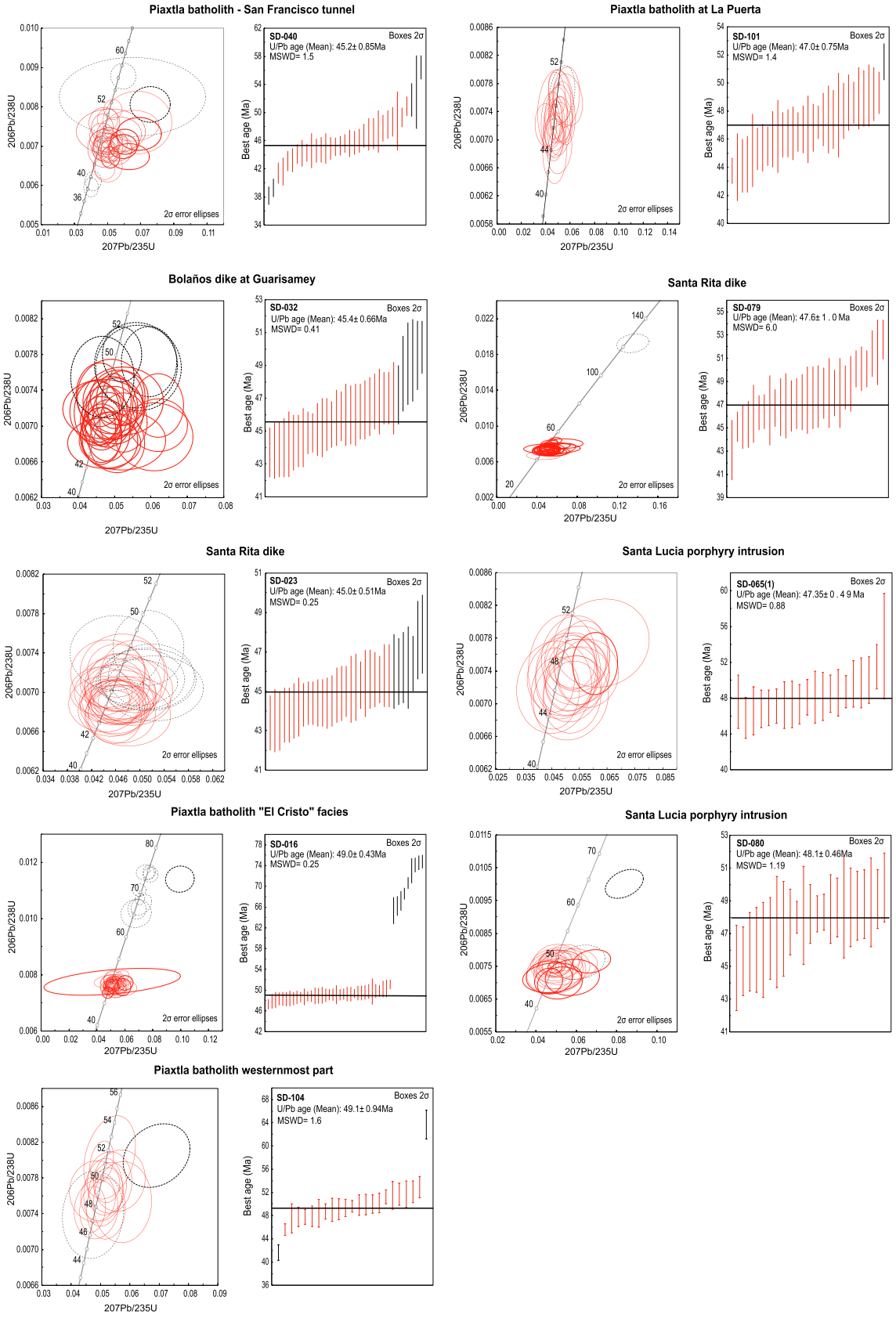

Fig. 7. Histograms and probability density diagrams for detrital zircons from the Las Palmas (upper panel) and Camichin (lower panel) continental sedimentary deposits, with indication of the main magmatic pulses in the San Dimas region.

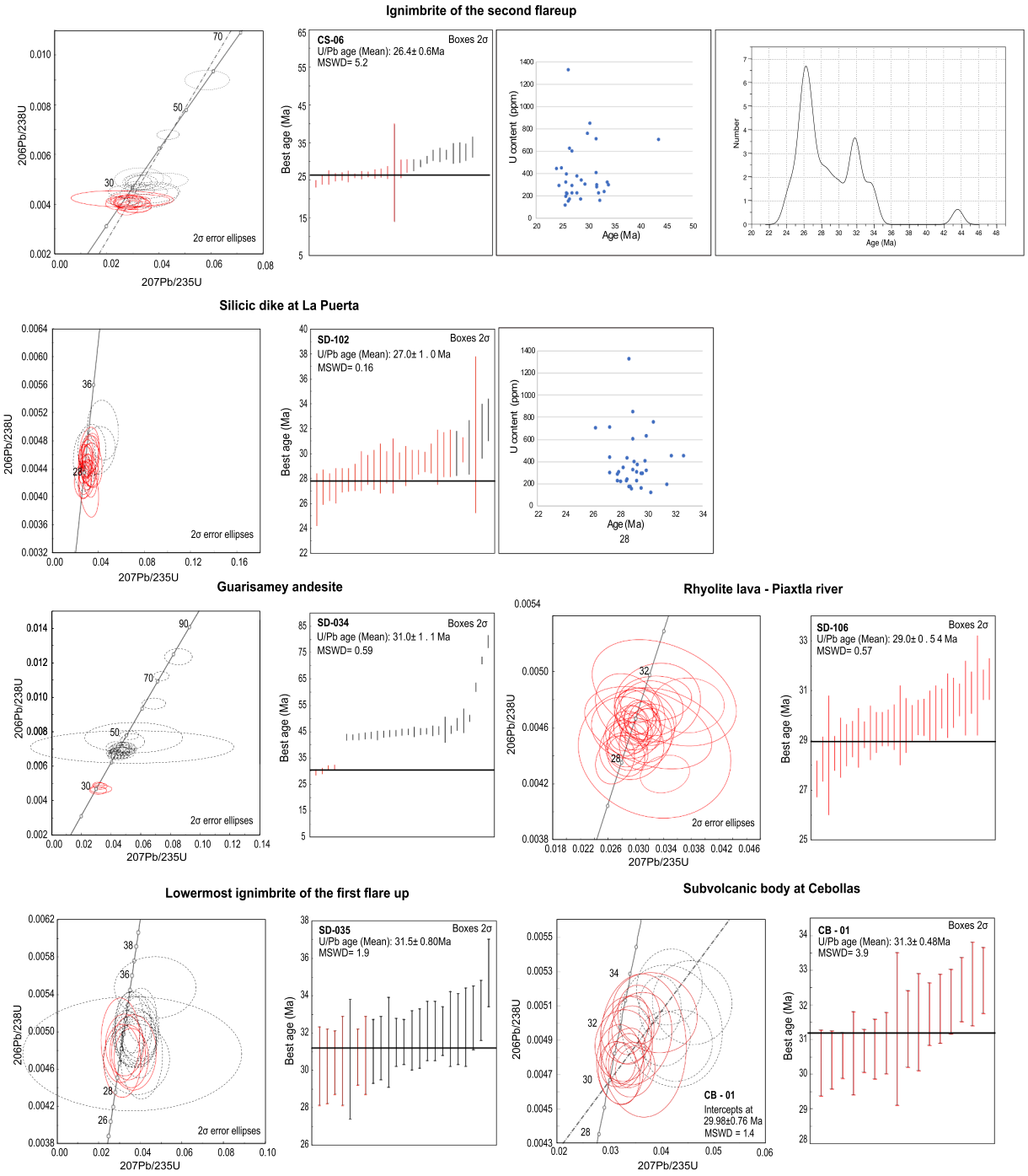

Fig. 8. Histograms and concordia diagrams of U-Pb ages for zircons of the Upper Volcanic Supergroup. Errors in calculated ages are 2σ. Black ellipses are data points not used in calculating the weighted mean.

056) (Fig. 5). The latter sample displays a wide range of grain ages from 69 to 82 Ma.

The Buelna member is a sequence of intermediate lavas characterized by porphyritic-fine texture and bedding, which commonly contain anhedral to subhedral crystals of plagioclase > quartz > hornblende > biotite in a groundmass of fine plagioclase. This member crops out throughout the district on top of the Socavón member with a thickness ranging from 20 to 100 m. One sample from the type locality yielded an age of 69.8 ± 0.85 Ma (SD 014-2) (Fig. 5).

The Portal member is a sequence of rhyolite flows and tuffs with a lithic-rich layer at the base and a thickness of 50–250 m. It contains anhedral crystals of quartz > plagioclase > biotite in a fine-grained sericitized groundmass. We obtained an age of 69.0 ± 1.7 Ma (SD 049) (Fig. 5) for a sample of the Portal member from the interior of the mine.

Volcanic rocks lithologically similar to the Socavón member were mapped south of the San Dimas district (Fig. 3). The main outcrops are in the creek west of Causita and in the Presidio River valley in the Mala Noche mining area. Two samples from the Causita area (CAU 16 001, CS 01) and two more from drillings in the Mala Noche area (MN 14-24, MN 14-24b) yielded tightly clustered ages comprised between 77.7 ± 0.88 and 75.5 ± 1.0 Ma (Fig. 5, Table 1), which confirm the correlation with the Socavón member.

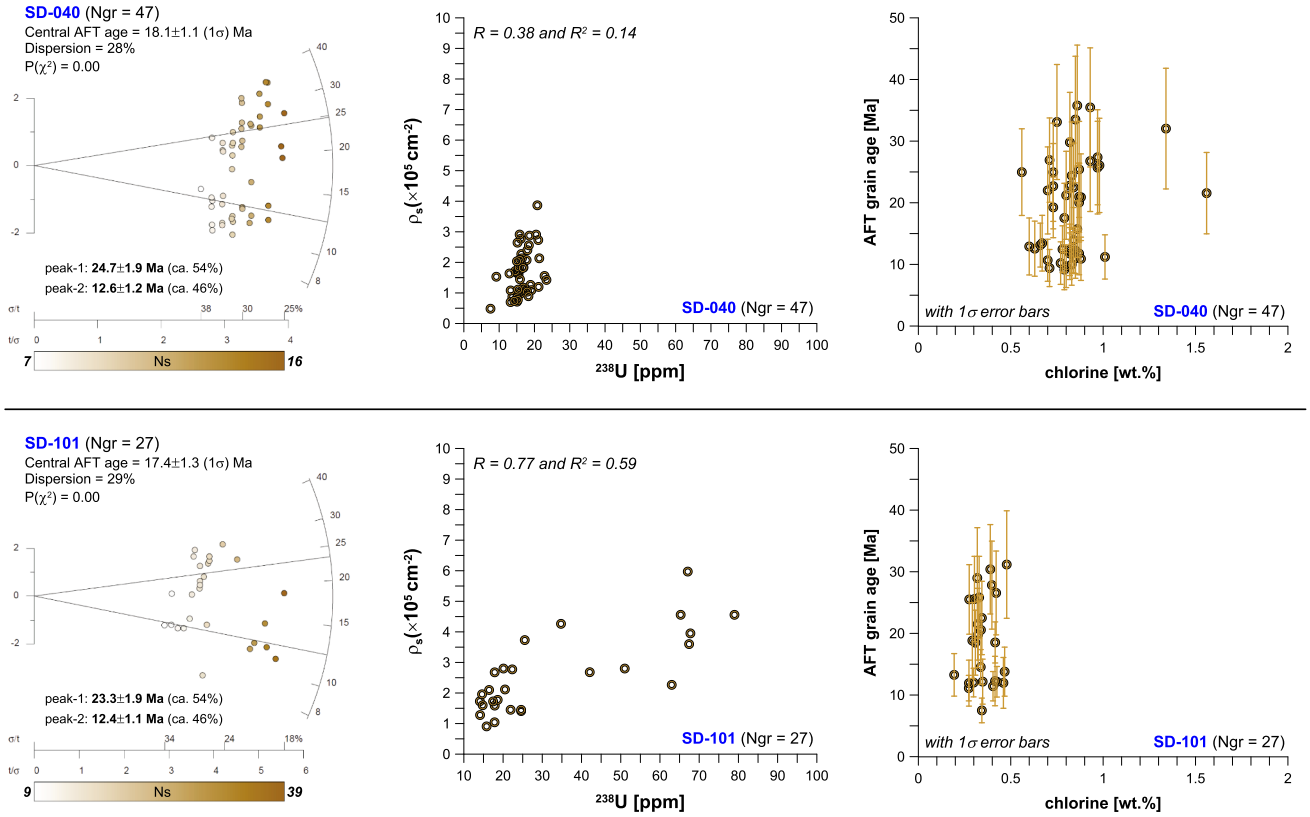

Fig. 9. Apatite fission-track results for samples SD-040 and SD-101. Radial plots were constructed using RadialPlotter of Vermeesch (2009). Ngr – number of apatite grains dated; P(χ^2) – chi-squared probability test; Ns – number of spontaneous tracks counted to calculate the track densities in individual apatites. The track density (ρ_s) versus ^{238}U concentration (analogue to isochron) and the single-grain age versus Cl content diagrams are also presents.

4.2.2. San Ignacio batholith

Our new Late Cretaceous ages for the lower volcanic succession at San Dimas make them coeval with the intrusive assemblage forming the San Ignacio granodiorite as defined by Henry et al. (2003), which is exposed west of the district along the Piaxtla river in the homonymous area (Fig. 2). Along the riverbed the batholith is clearly distinguishable from the younger Piaxtla batholith for its pervasive alteration and a more mature erosional landscape. The dominant lithology is a medium-grained equigranular granodiorite which contains anhedral biotite, hornblende, and clinopyroxene. We have dated one sample from the eastern part of the batholith, 16 km east of San Ignacio obtaining an age of 64.2 ± 0.9 Ma (SD 107) (Fig. 5), which is in line with previous K–Ar ages reported by Henry et al. (2003).

4.2.3. Andesite group

Andesitic subvolcanic bodies and lava flows are found intruding and covering, respectively, the Late Cretaceous succession of the San Dimas district with a cumulative thickness comprised between 200 and 850 m. Observations in mine interior indicate that the group display a range of texture without intrusive contacts between them. The sequence commonly starts with an andesite lava agglomerate with a fine texture, rich in lithic fragments ("Productive andesite"), which passes transitionally to a porphyritic texture ("Intrusive andesite") and then to a granular texture ("Arana diorite"). Regardless of the texture the andesite group is normally composed by plagioclase > hornblende > pyroxene > quartz ± biotite in an aphanitic groundmass (Fig. 11). Due to high hydrothermal alteration, these andesite bodies could not be dated by the ^{40}Ar–^{39}Ar method and because of their chemistry, zircon crystals are very rare. After several attempts we could separate a few zircons, which yielded a ~63 Ma age. Although insufficient to provide a statistically robust age, this value is consistent with the stratigraphic position of the Andesite group. Porphyritic andesite intrusions, composed by medium to fine crystal of plagioclase > quartz > biotite > hornblende > pyroxene and chlorite in a fine plagioclase groundmass cut the andesite group in the Santa Lucia mine. We have dated two of these bodies (SD 065-1, SD 080), which yielded indistinguishable ages of ~48 Ma. These crosscutting relationships and the few dated zircons indicate that the andesite group was emplaced in the Paleocene-early Eocene time span.

4.2.4. Piaxtla intrusive complex

Intrusive bodies of dioritic, granodioritic and granitic composition were grouped into the Piaxtla intrusive complex. This intrusive complex is part of a batholith well exposed in the Piaxtla river that intrudes the lower volcanic succession and the Andesite Group. The Piaxtla intrusive rocks present a wide range of texture, from equigranular to porphyritic (in dikes). The dominant lithology consists of medium to coarse grained granite to granodiorite. The oldest body, called "El Cristo granite", is exposed just south of the Piaxtla River near Tayoltita (Fig. 3). El Cristo is a fine-grained granite rich in K-feldspar that yielded an age of 49.0 ± 0.43 Ma (SD 016) (Fig. 6). A similar age of 49.1 ± 0.94 Ma was obtained in the westernmost part of the batholith along the Piaxtla river (SD 104) (Fig. 6). The main Piaxtla body consists of a medium to coarse grained granite with quartz > plagioclase > feldspar > biotite, but richer in pyroxene and hornblende. Two samples taken ~8 km apart gave slightly different ages of 47.0 ± 0.75 Ma and 45.2 ± 0.85 Ma (SD 101, SD 040), with the older age belonging to the westernmost sample (Fig. 6).

Several dike families associated with the Piaxtla batholith cut the Late Cretaceous volcanic succession, the Andesite Group and, sometimes, the main Piaxtla body. Although they are known by different names they have similar crosscutting relationships, intermediate composition, and only differ in texture and relative mineral abundances. The Santa Lucia dikes are exposed in the Santa Rita mine intruding E-W

Table 2
Petrography summary.

Sample	Geologic unit and location	Long. W	Lat. N	Elevation (m asl)	Rock type	Age (Ma)	Petrography description
Sierra Madre Occidental silicic large igneous province – Upper Volcanic Supergroup							
CS-06	Second flare-up. First ash flow above a conglomerate covering tilted ignimbrites at Causita	105°46′45.08″	24°0′47.72″	2595	Ash flow tuff	26.2 ± 0.29	Ash flow tuff. Sequential porphyritic texture, hialocrystaline with subeuhedral crystals of quartz (84%) > plagioclase (An 9%) > feldspar (Alk + Alb 7%) > biotite in a vitreous matrix. Clasts of andesite ignimbrite with epidote alteration and andesite ignimbrites with sericite and pyrite alteration. Strong sericite alteration overpirnted by epidote and Fe oxides in clasts. Two types of pyrites are presented, fine and coarse grain less than 1%.
SD-102	Silicic dike intruded by mafic dike, riverbed near La Puerta	106°00′23.57″	24°04′4.45″	415	Silicic pyroclastic dike	27.6 ± 1.00	Dacite pyroclastic dike. Sequential porphyritic texture, hialocrystaline and anahedral crystals of quartz (53%) > biotite > plagioclase (An 32%) > feldspar (Alk + Alb 15%). Strong pervasive sericite alteration. Two types of pyrites are presented: coarse and fine grain both less than 1%.
SD-106	Silicic lava near riverbed. Road Tayoltita to San Ignacio	106°08′14.40″	23°59′31.23″	290	Porphyritic rhyolitic lava	29 ± 0.54	Rhyolitic lava with quartz "eyes". Sequential porphyritic texture, holocrystaline and subeuhedral to anahedral crystals of quartz (70%) > feldspar (Alk + Alb 17%) > plagioclase (An 13%) > biotite. Strong diseminated sericite alteration overpirnted by pervasive moderated epidote. Two types of pyrite were found: 1) palid coarse grain (< 0.01%) and fine grain (< 0.01%). Overgrown quartz textures are present
CB-01	Shallow intrusion just north of Cebollas, below ignimbrites	105°48′20.94″	24°42′46.02″	1200	Fine-grained, hb-rich syenite	31.2 ± 0.43 30 ± 0.76	Syenite. Coarse to medium grain, equigranular texture, holocrystaline and anahedral crystals of feldspar (Alk + Alb 58%) > plagioclase (An 22%) > quartz (19%) > hornblende. Strong pervasive alteration of epidote, sericite and weak chlorite and calcite. Medium grain sphalerite is presented (< 3%) with fine pyrite inclutions (< 2%), Fe oxides were also found.
SD-034	Guarisamey andesite member right above SD 035. Piaxtla river east of Guarisamey	105°53′10.53″	24°08′21.87″	600	Porphyritic latite basaltic lava	31 ± 1.1	Latite basaltic lava. Porphyritic texture, holocrystaline of subeuhedral plagioclases (An 74%) > feldspar (Alk + Alb 23%) > quartz (3%) in a microcrystaline matrix (30%) with Fe oxides. Moderated sericite and biotite alteration in crystals and weak calcite. Fine anahedral pyrite is presented less than 1%. Broken crystals of plagioclase and quartz are presented.
SD-035	First volcanic unit above sedimentary unit. Piaxtla river east of Guarisamey	105°53′9.43″	24°08′13.25″	595	Reddish ignimbrites with plag, san, qz	31.5 ± 0.80	Reddish rhyodacite ignimbrite. Porphyritic texture, hialocrystaline with anahedral crystals of feldspar (Alk + Alb 40%) > plagioclase (An 31%) > quartz (29%). Strong pervasive sericite alteration overprinted by moderated chlorite and weak calcite. Two types of pyrite are presented: 1) fine grain in matrix (< 3%) and 2) coarse grain asociated to coarse quartz (< 1%). Coarse chalcopyrite is also presented less than 1%
Volcano-sedimentary unit							
SD-029	Camichin unit, road Tayoltita to Guarisamey	105°54′20.58″	24°07′19.07″	975	Lithic tuff	43.2 ± 2.30	Lithic tuff. Lithic fragments of porphyritic andesites, traquite andesites, rhyolites and sedimentary rocks inmerse into a vitreous matrix. Strong sericite alteration in matrix. Coarse grain pyrite is presented less than 1% associated to the lithic fragments.
SD-031	Palmas Formation, road Tayoltita to Guarisamey	105°54′16.28″	24°07′26.96″	965	Lithic arkose	52.1 ± 1.40	Lithic arkose. Detritic rock with clastic texture in a feldspar cement. Sandstone grain size of feldspar > lithic fragments > quartz. Sub-rounded to rounded clasts and inmadure. Lithic fragments of porphyritic andesites, felsic intrusions, volcanic and sedimentary rocks. Strong pervasive alteration of sericite, chlorite, epidote.
Lower Volcanic Complex							
Piaxtla intrusive suite							
SD-023	"Santa Rita"-type dike cutting Piaxtla batholith, 3 km west of Tayoltita	105°56′50.26″	24°05′08.30″	543	Porphyritic andesite with plag, hb, bio and qz	45 ± 0.51	Porphyritic andesite. Porphyritic texture, holocrystaline and subeuhedral crystals of plagioclase (An 57%) > feldspar (Alk + Alb 29%) > quartz (14%) > hornblende > biotite in a microcrystaline matrix of plagioclase. Strong alteration in crystals of sericite overprinted by moderated biotite and weak calcite and chlorite. Broken coarse pyrites are less than 1%. Overgrown quartz and graphic textures are present
SD-032	"Bolaños"-type dike cutting Piaxtla batholith, road to Guarisamey, 3 km east of Tayoltita	105°54′08.25″	24°07′43.96″	790	Porphyritic dacite with qz, plag, hb	45.4 ± 0.66	Porphyritic dacite. Sequential and porphyritic texture, holocrystaline and anahedral crystals of plagioclase (An 53%) > quartz (25%) > feldspar (Alk + Alb 22%) > hornblende in a microcrystaline matrix of silice. Strong pervasive sericite

(*continued on next page*)

Table 2 (*continued*)

Sample	Geologic unit and location	Long. W	Lat. N	Elevation (m asl)	Rock type	Age (Ma)	Petrography description
							alteration overprinted by moderated chlorite in crystals. Coarse euhedral pyrite is less than 1%.
SD-040	Piaxtla batholith, San Francisco tunnel	105°55′49.24″	24°06′36.25″	463	Coarse grained granite with qz, plag, bio, hb, px	45.2 ± 0.85	Coarse grain granite. Coarse equigranular texture, holocrystaline and subeuhedral crystals of quartz (46%) > feldspar (Alk + Alb 30%) > plagioclase (An 24%) > biotite > hornblende. Two events of plagioclase and biotite are presented: 1) with alteration, 2) without alteration. Strong alteration in crystals of sericite is overprinted by moderated calcite and chlorite. Accesory minerals, apatite, zircon and opaques. Coarse euhedral pyrite and chalcopyrite are presented. Overgrown quartz and graphic textures are present
SD-101	Piaxtla batholith, riverbed at La Puerta	106°00′29.15″	24°04′17.85″	417	White, coarse grained granodiorite with qz, plag, feld, hb, px, bio	47 ± 0.75	Coarse grain granodiorite. Coarse equigranular texture, holocrystaline and subeuhedral crystals of plagioclase (An 44%) > quartz (42%) > feldspar (Alk + Alb 13%) > biotite > anfibol. Weak pervasive sericite and chlorite alteration. Coarse pyrite less than 1%. Overgrown quartz and graphic textures are presented.
SD-079	Porphyritic andesite, “Santa Rita” dike, Santa Rita mine near entrance fo the main tunnel.	105°54′16.77″	24°07′11.02″	800	Porphyritic rhyodacite	47.5 ± 0.93	Porphyritic rhyodacite. Sequential porphyritic texture, holocrystaline with anahedral crystals of plagioclase (An 38%) > quartz (31%) > feldspar (Alk + Alb 31%) > piroxene > anfibole. Strong pervasive sericite and chlorite alteration overprinted by moderated epidote and weak calcite. Coarse euhedral pyrite is less than 0.1%.
SD-065(1)	Porphyritic dacite, “Santa Lucia” dike, San Luis tunnel between Santa Lucia and San Salvador veins	105°58′21.58″	24°08́11.27″	799	Porphyritic rhyodacite	48 ± 0.67	Porphyritic rhyodacite. Sequential porphyritic texture, holocrystaline with subeuhedral crystals, from coarse to Medium grain, of quartz (54%) > feldspar (Alk + Alb 30%) > plagioclase (An 15%) > piroxene > anfibol > biotite. Strong diseminated sericite alteration overprinted by moderated chlorite, epidote alteration and weak calcite. Coarse euhedral pyrite is presented less than 5%.
SD-080	fPorphyritic andesite, “Santa Lucia” dike, San Luis tunnel between Santa Lucia and San Salvador veins	105°58′21.58″	24°08́11.27″	799	Porphyritic quartzomonzonite	48 ± 0.46	Porphyritic quartzomonzonite. Sequential porphyritic texture, holocrystaline with anahedral crystals of plagioclase (An 46%) > feldspar (Alk + Alb 35%) > quartz (18%) > biotite > piroxene > anfibole. Strong diseminated sericite and chlorite, moderated epidote and weak calcite alteration. Fine euhedral pyrite is less than 0.1%.
SD-016	Piaxtla batholith, “El Cristo” facies, near entrance of the tunnel. Intrusive contact with Socavón member	105°56′15.30″	24°05′34.96″	573	Fine grained granite with qz, alk feld, plag, hb	49 ± 0.43	Fine grain granite. Fine equigranular texture, holocrystaline with crystals of quartz (40%) > feldspar (Alk + Alb 34%) > plagioclase (An 26%) > hornblende. Moderated pervasive sequndary biotite overprinted by weak sericite, chlorite and epidote. Fine and coarse pyrite are presented less than 1%. Overgrown quartz textures are presented.
SD-104	Piaxtla batholith, riverbed 7 km west of La Puerta	106°03′44.40″	24°02′20.50″	350	Medium grained granodiorite with qz, plag, bio, hb	49.1 ± 0.94	Granodiorite. Medium equigranular texture, holocrystaline with crystals of quartz (49%) > plagioclase (An 36%) > feldspar (Alk + Alb 16%) > biotite > anfibole. Weak pervasive chlorite, sericite and calcite alteration. Coarse euhedral pyrite was found less than 0.3%.
Sinaloa batholith							
SD-107	Sinaloa batholith, 16 km east of San Ignacio. Locally completely altered to unconsolidated sand	106°16′9.50″	23°57′17.83″	253	Medium grained granodiorite	64.16 ± 0.90	
Tarahumara formation							
SD-049	Portal member. San Jose tunnel, recess 598	105°59′53.92″	24°07′26.12″	878	Lithic rhyodacite ignimbrite	69 ± 1.70	Lithic rhyodacite ignimbrite. Porphyritic texture, hialocrystaline with subeuhedral to anahedral crystals (20%) of quartz (47%) > feldspar (Alk + Alb 27%) > plagioclase (An 26%) > biotite. Angular clasts of coarse and tabular porphyritic andesites and agregates of quartz. Strong sericite in crystals, moderated calcite and weak chlorite in halos around crystals. Fine euhedral pyrite is less than 1%.
SD-014(2)	Buelna member, 4 km SSW of San Dimas	105°58′15.89″	24°07′05.51″	665	Porphyritic andesitic lava	69 ± 0.85	Porphyritic andesitic lava. Sequential porphyritic texture. Holocrystaline with anahedral to euhedral crystals (30%) of plagioclase (An 61%) > feldspar (Alk + Alb 29%) > quartz (10%) > hornblende > biotite in a afanitic matrix of tabular plagioclases (70%). Weak pervasive chlorite, sericite and epidote. Coarse Py less than 1%.
SD-056		105°59′50.07″	24°06′51.79″	620	Porphyry rhyodacite	73 ± 1.5	

(*continued on next page*)

Table 2 (*continued*)

Sample	Geologic unit and location	Long. W	Lat. N	Elevation (m asl)	Rock type	Age (Ma)	Petrography description
	Porphyry intrusion within the Socavón member, stream at the Sinaloa-Durango border						Porphyry rhyodacite. Holocrystaline with anahedral crystals (30%) of quartz (58%) > feldspar (Alk + Alb 25%) > plagioclase (An 17%) > biotite in a afanitic matrix (70%) of quartz (60%) and feldspar (10%). Strong pervasive sericite alteration in matrix, moderate turmaline and chlorite alteration in crystals and weak calcite. Two events of mineralization are presented (less than7%): 1) coarse grain of Py, Cpy, Ga, Sph and 2) fine grain of Cpy, Ga, Sph. Overgrown quartz textures are presented.
SD-004	Socavón member, Tayoltita to San Dimas road	105°55′49.12″	24°08′08.39″	1176	Lithic porphyritic rhyolitic lava	75 ± 0.77	Lithic porphyritic rhyolitic lava. Holocrystaline with anahedral to sub euhedral crystals (65%) of feldspar (Alk + Alb 57%) > quartz (31%) > plagioclase (An 12%) > hornblende > biotite in a microcrystaline matrix (35%). Rounded clast of andesites and rhyolites. Strong pervasive sericite alteration overprinted by moderate chlorite and weak calcite and turmaline. Three types of pyrite are presented: 1) broken coarse Py (less than1%), 2) fine elongate Py (less than1%) and 3) very fine anahedral Py (less than3%). Overgrown quartz textures are presented.
SD-020	Socavón member, near Piaxtla river 2 km west of Tayoltita	105°56′49.18″	24°05′23.49″	570	Quartz latite lava	75.4 ± 0.8	Quartz latite lava. Porphyritic texture, holocrystaline with medium crystals (90%) of plagioclase (An 57%) > feldspar (Alk + Alb 37%) > piroxene > anfibole > biotite > quartz (7%) in a afanitic plagioclase matrix (10%). Moderate sericite and chlorite alteration in crystals. Two types of pyrites are presented: 1) fine anahedral grains (less than1%) and 2) very fine pyrite in inclutions in the former pyrite (less than1%), coarse anahedral chalcopyrite is also presented less than 1%.
MN-14_24b	Mala Noche drillhole. This rock is observed intruding the whole drilling	105°44′47.981″	23°54′15.923″	1038	Px-rich porphyritic quartz latite	75.5 ± 1.0	Porphyritic quartz latite. Holocrystaline, medium to fine anahedral crystals of feldspar (Alk + Alb 45%) > plagioclase (An 37%) > quartz (18%) > piroxene > biotite. Strong pervasive sequndary biotite alteration overprinted by moderate pervasive calcite and sericite. Coarse anahedral pyrite is presented less than 3% and Fe oxides in pots. Quartz rapakibi texture was found.
MN-14_24	Mala Noche drillhole.	105°44′47.95″	23°54′15.906″	950	Andesitic lava	76.06 ± 0.63	Andesitic lava. Sequential porphyritic texture. Holocrystaline with sub euhedral to anahedral crystals of plagioclase (An 81%) > feldspar (Alk + Alb 13%) > quartz (7%) > hornblende in a matrix of fine anahedral plagioclase. Strong pervasive calcite alteration overprinted by moderated sericite and chlorite. Coarse anahedral pyrite is less than 4%, Fe oxides lower than 1%. Overgrown quartz textures are presented.
CAU-16_001	Causitas drillhole. This rock includes clast of the whole sequence. Dated as detrital	105°46′56.21″	24°0′58.24	2358	Lithic rhyodacite lava	76.5	Lithic rhyodacite lava. Sequential porphyritic texture. Holocrystaline with anahedral crystals of quartz (61%) > feldspar (Alk + Alb 23%) > plagioclase (An 16%) > biotite in a microcrystaline quartz matrix. Rounded lithic fragments of andesites and quartz agregates. Strong pervasive sericite alteration is overprinted by moderate chlorite and calcite alteration. Coarse euhedral pyrite and Fe oxides are less than 2% pervasive. Overgrown quartz textures are presented.
CS-01	Lava hosting the an epithermal vein at Causita.	105°46′58.50″	24° 0′59.08″	2518	Lithic rhyodacite ignimbrite	77.73 ± 0.88	Lithic rhyodacite ignimbrite. Caotic porphyritic texture. Hialocrystaline with crystals of quartz (61%) > plagioclase (An 25%) > feldspar (Alk + Alb 15%) > biotite. Strong, pervasive sericite alteration. Rounded lithic clasts of quartz agregates. Coarse, euhedral pyrite is also present less than 1%.

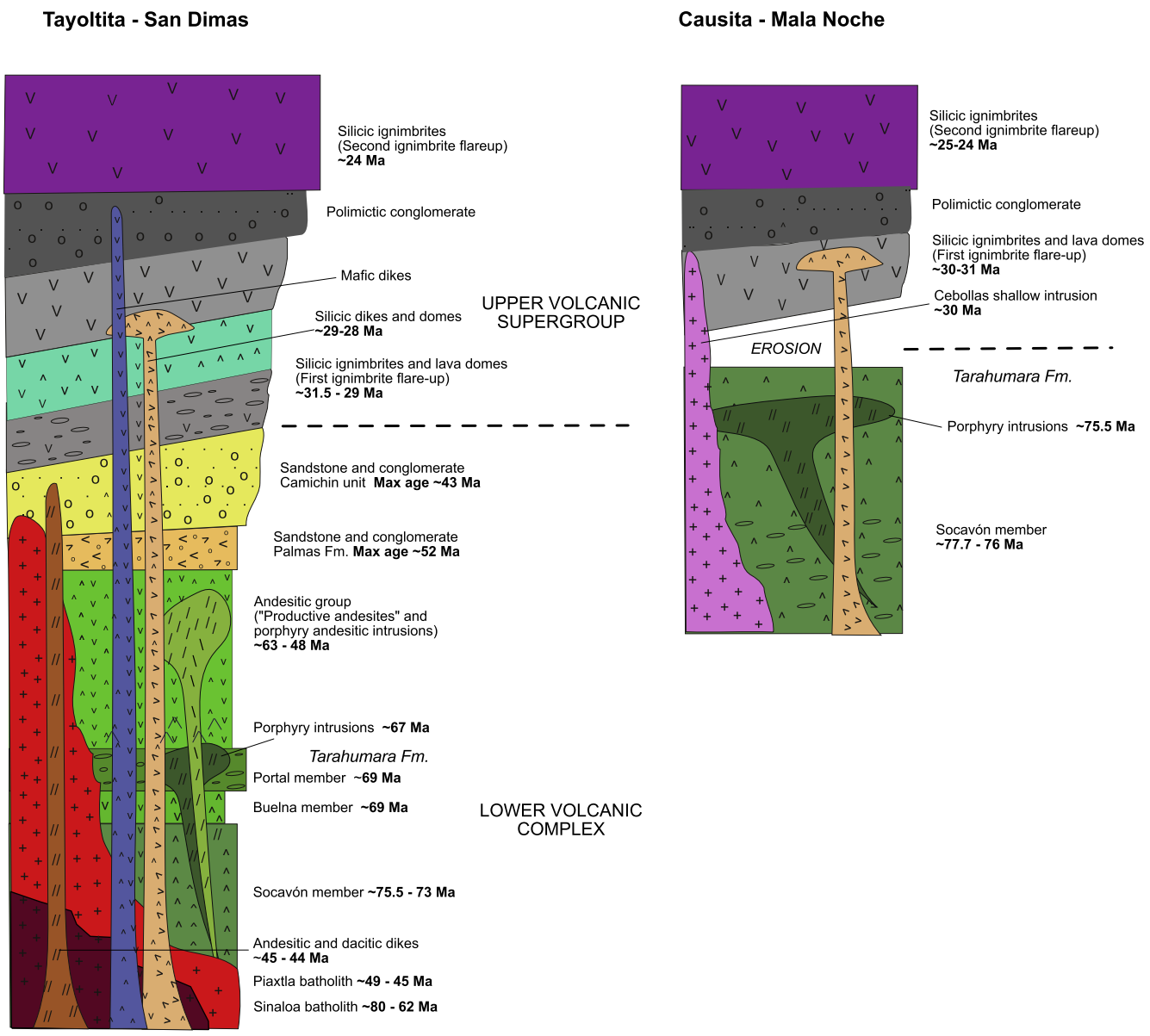

Fig. 10. New stratigraphic columns for the San Dimas and Causita-Mala Noche areas based on fieldwork and U-Pb geochronology presented in this work.

striking fractures that crosscut a massive porphyry andesite. The dike is a porphyritic andesite, composed of medium to fine phenocrystals of plagioclase > quartz > hornblende > pyroxene and biotite in a fine plagioclase groundmass. Santa Rita dikes are found in many areas of the district also intruding E-W striking fracture. They consist of porphyry andesite with medium to coarse phenocrystals of plagioclase > quartz, but richer in pyroxene and hornblende than the Santa Lucia. The Bolaños dikes are also intruded into E–W-striking fractures, have a dacitic composition and are also rich in pyroxene and hornblende, with the latter showing coarse phenocryst texture. The U-Pb age support the field observation that all these dikes belong to the same magmatic pulse as the Piaxtla batholith, with the Santa Lucia slightly older than Santa Rita and Bolaños dikes. As mentioned before two Santa Lucia dikes yielded ages indistinguishable within the error clustered at ~48 Ma (SD 065-1, SD 080) (Fig. 6). Samples from the Santa Rita dikes and Bolaños dikes also yielded identical ages (within error) of ~45 Ma (SD 32, SD 23) (Fig. 6).

4.2.5. Sedimentary formation

Two sedimentary formations have been recognized separating the LVC from the UVS. The Las Palmas formation is composed by conglomerates, sandstones, red beds and mudstones. The Las Palmas formation lies unconformably on the Andesite Group in eastern part of the district. The Camichin formation crops out in the eastern part of the district (Santa Rita mine and Guarisamey area), ranging in thickness between 50 and 300 m. It has been described as an alternating sequence of andesitic tuffs and volcano-sedimentary deposits, but in the field, we only observed the latter lithology. We have dated detrital zircons from both units (Fig. 7). For the Las Palmas formation (SD 031) we obtained a maximum age of deposition of 52.1 ± 1.4 Ma with peaks at ~56 and ~64 Ma. A sample from the Camichín formation previously mapped as a tuff turned out to be a sandstone (SD 029), which yielded a maximum depositional age of 43.2 ± 2.3 Ma with a major peak at ~56 Ma. These peaks in detrital zircons age at the beginning and end of Paleocene point to important magmatic pulses that will be discussed later.

4.2.6. Upper volcanic supergroup

Unconformably covering the continental sedimentary formations and the Andesite Group are two packages of silicic ignimbrites and domes, with intercalation of minor amount of mafic lavas, fed by dikes

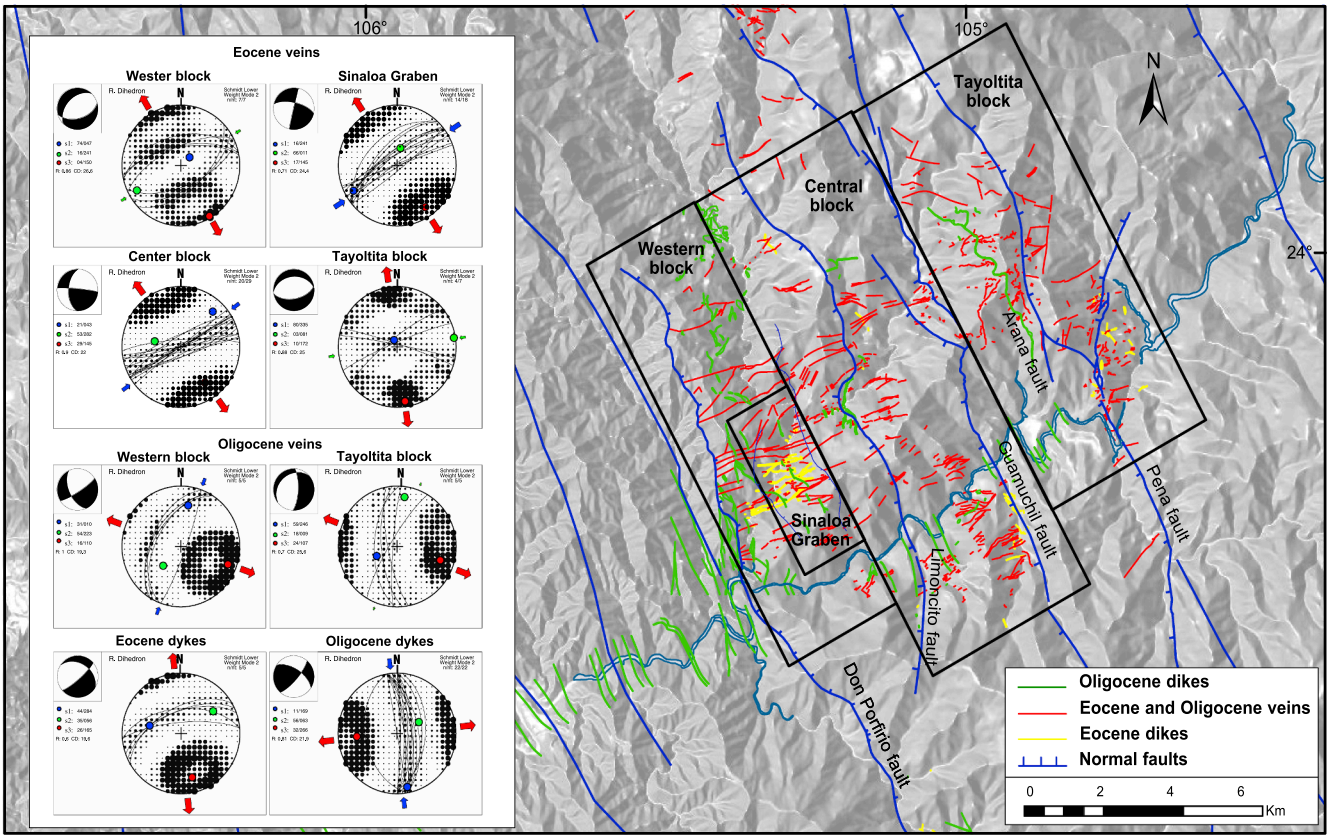

Fig. 11. Structural map of San Dimas mining district showing the mains fault systems, veins, and dikes, with stereograms showing their orientation (lower hemisphere).

of bimodal composition. A volcanic conglomerate and an angular unconformity separate the two packages. The base of the UVS is clearly exposed along the Piaxtla River near Guarisamey, where the homonymous member it is composed by a rhyolitic ignimbrite and a series of andesitic lavas. The ignimbrite contains feldspar > plagioclase > quartz as the main crystals in the glassy matrix. The andesite lavas have a holocrystalline porphyritic texture with subhedral plagioclase phenocrystals and rare quartz. We obtained an age of 31.5 ± 0.8 Ma for the first ignimbrite capping the sedimentary formation (SD 035) and an age of 31.0 ± 1.0 Ma for the andesite agglomerate that lies just above (SD 034). This latter unit displays a large population of zircons with ages of the Piaxtla intrusive suite, which were considered as inherited xenocrystals (Fig. 8). Despite being based on four crystals only, we consider our U/Pb age reliable since the andesite flow lies in direct contact with the ignimbrite dated 31.5 Ma and no paleosoil was observed in between. The difference with the ~24 Ma K–Ar age reported by Enríquez and Rivera (2001b) for this unit is likely due to the fact that the andesite is highly altered, which may have resulted in Ar loss. A shallow granitic intrusion 10 km to the SSE of Guarisamey yielded an age of 31.3 ± 0.50 Ma (CB 01), which suggests it represents an intrusive equivalent of the first ignimbrite package. Henry et al. (2003) reported similar K–Ar dates on biotite for a granodiorite and a quartz diorite dike about 10 km to the north, in the Piaxtla river valley. Rhyolitic domes that cover the flat-lying ignimbrite succession NE of San Dimas are undated. However, we have dated a rhyolite flow that rest unconformably over the San Ignacio batholith west of the district at 29 ± 0.54 Ma, an age very similar to that obtained by K-Ar by McDowell and Keizer (1977) and by U/Pb by Ferrari et al. (2013) for the massive rhyolite dome of Las Adjuntas, located 55 km southeast of San Dimas.

NNW–SSE-striking felsic and mafic dikes cut most of the succession of the district. The felsic dikes are locally known as “Rebo” and consists of pyroclastic intrusions rich in quartz > plagioclase > biotite in a glassy matrix. These dikes are particularly abundant in the proximity of the fault system at the western limit of the district (Don Porfirio fault) at La Puerta (Fig. 11). A sample from one of these dikes at this location yielded an age of 27.0 ± 1.0 Ma (SD 102) (Fig. 8). The mafic dikes are locally known as “San Luis” and consist of basaltic lavas with porphyritic texture and plagioclase phenocrystals in a microlithic groundmass. The K-Ar age of 29.5 ± 0.7 Ma reported by Henry and Fredrikson (1987) for an andesitic dike west of the district is probably representative for these intrusions. For the ignimbrite succession that cover the Oligocene ignimbrites in angular unconformity we obtained an age of 26.2 ± 0.29 Ma. For this sample, we exclude a Pb loss as there is no correlation between higher U content and younger ages (Fig. 8). In addition, this sample belongs to an ignimbrite overlaying a conglomerate and lays in angular unconformity with the first ignimbrite package. The slightly older age obtained with respect to the correlative El Salto-Espinazo del Diablo succession (24–23.5 Ma; McDowell and McIntosh, 2012) may be due to subtle zircon inheritance in the form of antecrysts, as it is quite common for this ignimbrite package in other part of the Sierra Madre Occidental (Bryan et al., 2008; Ferrari et al., 2013). Enríquez and Rivera (2001b) report a K–Ar age of 20.3 ± 0.8 Ma for the uppermost ignimbrite of the capping sequence NW of Guarisamey (Fig. 3). This age, obtained on plagioclase, is uncommon for the region, where the second ignimbrite flareup only consist of the 24–23.5 Ma El Salto–Espinazo del Diablo succession. The younger age can be due to Ar loss, taking into account that the closure temperature of plagioclase can be as low as 200 °C (e.g. Cassata and Renne, 2013).

5. Tectonics

As described in Section 2.2, the tectonic setting of the San Dimas district is dominated by major tilted blocks separated by NNW striking normal fault system that expose the mineralization (Fig. 10). The Limoncito, Guamuchil, and the Arana faults, located in the central and eastern part of the district, dip to the WSW with inclination varying from 80° to 55°, the Don Porfirio fault dip toward the ENE with a high angle and the Peña fault is almost vertical. Rocks in the Tayoltita and Central blocks are typically tilted 30–35° to the ENE, whereas in the Western block they are tilted 10–15° to the WSW. Most mineralized veins (61 mapped structures) strikes E–W to ENE–WSW, with only a few in the easternmost part of the district (Tayoltita block) striking ~N–S (5 mapped structures) and in the western block striking NNE–SSW (5 mapped structures) (Fig. 10).

The E–W to ENE–WSW striking veins formed before the Oligocene, as they do not cut the UVS and are exposed by the NNW striking normal fault systems. However, they almost did not change their inclination because are approximately orthogonal to the tilting. These veins cut the Late Cretaceous volcanic succession and the Andesite group, and some also cut the oldest part of the Piaxtla batholith (El Cristo granite) dated at ~49 Ma. Based on these crosscutting relations the veins can be limited to the late Eocene. Our ~45 Ma ages for the "Santa Rita" and "Bolaños" dikes (Table 1), whose strike is parallel to the veins, suggest that they could be part of the same episode. Recent Ar–Ar dating of adularia (Enriquez et al., 2018) points to a slightly younger age of ~41 Ma. The associated stress regime would have been characterized by NW–SE σHmin and NE-SW σHmax, with a possible transtensional deformation regime in some areas, as observed by Horner and Enriquez (1999) (Fig. 10).

NNW striking normal faults and block tilting post-date the first ignimbrite package of the UVS. However, the angular unconformity and the conglomerate that separate it from the second ignimbrite package indicate that faulting occurred between ~30 and ~24 Ma, as it has documented in several areas of Sinaloa (Ferrari et al., 2013). This is also confirmed by the 27.0 ± 1.0 Ma age we obtained for a felsic dike intruded parallel to and in proximity of the NNW striking Don Porfirio fault system (Fig. 10) (SD 102, Table 1). Taking into account this age, the crosscutting relations, and the fact that they are only moderately tilted, we consider NNW–SSE to N–S striking veins and dikes as emplaced during the initial stage of the Oligocene extension. Assuming that the veins and dikes were the result of a pure extensional opening, they would indicate an ~E–W to WNW–ESE extension regime (Fig. 10) that have been also reported for the western SMO at the beginning of the Gulf of California rift (Ferrari et al., 2013, 2017; Duque-Trujillo et al., 2015). Further west, the ignimbrite package of the second ignimbrite flareup is also tilted (Henry, 1989; Henry and Fredrikson, 1987; Henry and Aranda-Gómez, 2000), implying that a second extensional episode affected this area.

The result of AFT dating on two samples at different altitudes of the Piaxtla batholith provide further support to this multiple-stage extensional history (Fig. 9). The dated samples show consistent cooling ages with a first group of ages at the end of Oligocene (24.7 ± 1.9 and 23.3 ± 1.9 Ma) and a second one at the end of middle Miocene (12.6 ± 1.2 and 12.4 ± 1.1 Ma).

On a larger scale, our new mapping and absolute dating south of the district point to a major structure roughly parallel to the Piaxtla river. In fact, the Late Cretaceous volcanic succession lies at a maximum of ~1500 m of elevation in the San Dimas area whereas it crops out at ~2600 m in the Causita area to the SSE (Fig. 3). The easiest explanation for a difference of ~1100 m of elevation between the San Dimas and Causita blocks is the presence of a major ENE–WSW striking and NNW dipping normal fault system running somewhere in the Piaxtla river valley, here named Piaxtla fault zone. A structure with this orientation but opposite dip (i.e. down to the SSE) is drawn some km south-southeast of the river in the geologic map of Henry and Fredrikson (1987) but not described. In the field, no clear fault zone is observed in Piaxtla riverbed, which between Tayoltita and San Ignacio is always cut into the Piaxtla granite. We infer that this fault system is older than the ~32 to 30 Ma ignimbrites and thus buried beneath them. In Fig. 3 we draw this inferred normal fault system along the trace drawn by Henry and Fredrikson (1987) but we assume that it has an opposite displacement.

In the Tayoltita area the intrusion contact of the Piaxtla batholith in the NNW side of the valley has a lower elevation with respect to the SSE side, which suggest that the batholith may have intruded into a pre-existing normal fault zone. If extended toward the west the Piaxtla fault zone would limit a WSW-ENE trending horst of the pre-Laramide basement that crop out along the coast between Mesa Cacaxtla and Mazatlán but not to the north and to the south (Fig. 2). On a regional scale is very possible that other fault systems orthogonal to the Gulf of California may exists and controlled the segmentation of the rift in the following extensional stage. This structural grain may be inherited from even older deformation episodes. Henry (1986) reported ENE trending folds and thrust faults, orthogonal to the paleo-subduction zone in Jurassic to Early Cretaceous rocks in Sinaloa, that would have formed by oblique convergence prior to 100 Ma.

6. Discussion and conclusion

6.1. Revision of the San Dimas district stratigraphy

Our new ages and geologic observations provide tighter constraints on the magmatic and mineralization pulses in the San Dimas district and allow to correlate its stratigraphy with other regions of the SMO. One of the main contributions is the recognition of the presence of a Late Cretaceous volcanic activity in the area. Previous studies were unable to date the LVC succession. Some workers suggested that it was older than the Piaxtla intrusive complex (Henshaw, 1953; Nemeth, 1976; Henry and Fredrikson, 1987; Enríquez and Rivera, 2001b) but mostly Eocene in age, by correlation with andesites dated at 51.6 Ma south of Durango by McDowell and Keizer (1977). The ages of the Socavón, Buelna, and Portal members obtained in this work clearly demonstrate that these rocks are part of the Late Cretaceous magmatic episode of the so-called Laramide arc. In particular, they share the same time span, lithology and composition of the Tarahumara formation of Sonora (Wilson and Rocha, 1949; McDowell et al., 2001). As in Sonora this Late Cretaceous volcanic succession is exposed to the east of the age-equivalent Laramide batholiths (Fig. 2), which suggest a wider volcanic arc that was eroded toward the coast.

For the following Andesite group Enríquez and Rivera (2001b) reported ages between 38.8 and 36.6 Ma using the K–Ar method. Based on these ages, the authors linked the andesitic magmatism with the epithermal mineralization events, which produced similar ages (38.5–31.9 Ma). Given the widespread alteration of these rocks these ages are unreliable and contradicts our new U-Pb ages and crosscutting relations. In fact, we obtained a few zircons of early Paleocene age for the "Intrusive andesite" and, more importantly, two reliable U-Pb ages of ~48 Ma for intrusive bodies that cut the Andesite group. Therefore, we have relocated this group in the Paleocene to Early Eocene. In this context we consider that the K-Ar ages of Enríquez and Rivera (2001b) were the result of partial resetting of the dated minerals.

We observed that the Piaxtla intrusive complex intrude the whole LVC from the base to the top and was formed by different magmatic pulses, separated based on texture, composition and age. Our U/Pb age confirm earlier K–Ar and U/Pb ages (Enríquez and Rivera, 2001b; Henry et al., 2003) and show that the development of the batholith took place in several millions of years from ~49 to ~44 Ma. A novel contribution is the dating of the "Santa Rita" and "Bolaños" intermediate dikes, that were previously thought to be somewhat younger than the Piaxtla suite but turned out to be concurrent with the last intrusion stage. These ages are relevant because document a period of ~13 Ma

without any magmatic activity in the area, during which previous authors suggested the occurrence of a mineralization event.

The occurrence of the continental sedimentary Las Palmas and Camichín formations points to an early stage of extension with the formation of intermontane basins in the Eocene. The rock fragments and different zircon populations indicate that these clastic units were mostly derived from volcanic edifices (domes and compound volcanoes) that form the Andesite Group and, to a lesser extent, the Piaxtla intrusive suite, most likely the Santa Rita and Bolaños dikes. A continental sedimentary deposits lithologically equivalent to the Las Palmas formation and in the same stratigraphic position is reported south of the San Dimas district in the Mala Noche area (Servicio Geológico Mexicano, 2002), where it is called "Palmarito conglomerate". At a regional level it can be correlated with many discontinuous continental sedimentary deposits that mark a period of the erosion and low volcanic activity between the bulk of LVC and the UVS (McDowell and Keizer, 1977; McDowell and Clabaugh, 1979; Ferrari et al., 2007).

The new U/Pb ages for the base of the ignimbrite succession at San Dimas are consistent with those of the Durango sequence, whose Ar–Ar ages range from 31.7 to 29.9 Ma (McDowell and McIntosh, 2012). A slightly older age of 32.5 Ma was obtained by Ferrari et al. (2013) for a tilted ignimbrite sequence east of Mala Noche. This confirms that the eastward prolongation of the Durango sequence at least up to the Durango–Sinaloa state boundary.

6.2. Timing of igneous activity

Henry et al. (2003) interpret that igneous activity was mostly continuous between ~100 and 45 Ma in Sinaloa. Although at a regional level some ages of igneous bodies fall between ~61 and ~49 Ma and our detrital zircons show a peak in this age interval, along the Piaxtla river valley a distinction can be clearly made between the San Ignacio and the Piaxtla batholiths. Along the river, we observe a clear change in morphology (much less relief) and increase in alteration (intrusive rocks often reduced to sand) and mineral composition (mafic minerals more abundant) between the two batholiths. Ages also change rather abruptly (Fig. 2). The Piaxtla batholith is exposed for ~35 km to the northeast of the contact with ages restricted between 49.6 and 43.7 Ma, whereas the San Ignacio batholith has ages between ~67 and ~61 Ma to the southwest (Henry et al., 2003, this work). Supporting this inference, sample 199 of Henry et al. (2003), from what we mapped as the Piaxtla batholith, is a tonalite that yielded a biotite age of 49.3 ± 0.6 Ma; however, just 2 km to the south sample 152 of Henry et al. (2003) is a granodiorite that yielded a hornblende age of 67.1 ± 1.5 Ma. Interestingly, this same sample yielded a biotite age of 51.3 ± 0.6 Ma, a large difference of 16 Ma that cannot be due to normal cooling but rather to a thermal resetting of the biotite system due to the nearby Piaxtla intrusion. Our new ages also confirm a gap in igneous activity between ~43 Ma (youngest age of the Piaxtla intrusive suite) and ~32 Ma (first ignimbrite of the UVS), which is also marked by the deposition of the Las Palmas and Camichín sedimentary successions.

6.3. Implication for the mineralization events at San Dimas

A detailed structural, geochemical and geochronologic study of the vein system is the focus of a forthcoming paper. However, the data presented in this work provide some constraint on the mineralization events of the San Dimas district. San Dimas has been traditionally classified as a classic Au–Ag epithermal low sulfidation vein system developed during a single mineralization episode during in a late stage of the LVC magmatism (Henshaw, 1953; Smith and Hall 1974; Smith et al., 1982; Clarke, 1986; Clarke and Titley, 1988). Enríquez and Rivera (2001b) obtained similar Late Eocene K–Ar ages for andesitic intrusions and some of the veins, which led them to associate the two events and conclude that the mineralization occurred in the ~38 to 32 Ma time span. However, the minerals dated by these authors were adularia and feldspar, whose closure temperature for the K– Ar system (~150 to 200 °C; Love et al., 1998) is well below the temperature of the hydrothermal fluids circulating in the district (~260 °C; Clarke and Titley, 1988). This means that the late Eocene ages of Enríquez and Rivera (2001b) should be considered minimum ages, likely resulting from partial resetting.

In this work we have dated the main geologic units of San Dimas using zircon, whose closure temperature for the U/Pb system (~900 °C) is much higher than the temperature of any hydrothermal fluid. Our data place the Andesite Group into the Paleocene–early Eocene time span, as it is also confirmed by the age peaks in the continental sedimentary deposits of the Las Palmas formation. Although we did not directly date the mineralization, the most important magmatic event postdating the host rock of the Andesite Group is the Piaxtla intrusive suite, emplaced between ~49 and ~44 Ma, which we consider the most likely thermal source for the dominant ENE-WSW trending vein system. These veins occupied fractures and faults that developed before the first ignimbrite flare up of the UVS that may have also controlled the emplacement of the Piaxtla batholith. Recently, Enriquez et al. (2018) obtained Ar–Ar ages of 41 ± 0.2 and 37.8 ± 0.2 Ma on adularia from two veins of the E–W system with high Ag/Au ratio. The first age confirms the K–Ar age of 40.9 Ma on adularia from an undefined mine at Tayoltita obtained by Henry et al. (2003). The new Ar–Ar ages show a well-defined plateau, and indicate that at least part of the Ag/Au mineralization occurred ~3 to 6 Ma after the emplacement of the Piaxtla intrusive suite.

On the other hand, NNW–SSE to N–S veins emplaced in the eastern part of the district must be associated with the similarly oriented normal faults responsible for the block tilting in the San Dimas area. As mentioned in the previous section, these extensional faults are partly coeval with the silicic volcanism of the flare up dated at ~32 to 29 Ma. If this is the case, the NNW–SSE to N–S veins should differ from the rest of the district in term of Ag/Au ratio and other structural and chemical features. In conclusion, the data presented in this work show that the San Dimas district was developed during multiple mineralization events tied to magmatic and tectonic pulses that affected the central part of the Sierra Madre Occidental.

Acknowledgements

This research is part of the PhD project of the first author at Universidad Nacional Autónoma de México (UNAM) Postgraduate Program and was funded by Consejo Nacional de Ciencias y Tecnología (CONACYT), Mexico, Grant CB 237745-T to L. Ferrari. We thank Primero Mining (presently First Majestic Silver Corp.) for sharing unpublished information and for logistical support. We thank Chris Henry for his thorough review that contribute to clarify several aspects of the work and two anonymous reviewers that helped to improve its presentation. A special thanks to Nicolas Landón for his strong support in the initial phase of the research and to Miguel Pérez for sharing his knowledge of the ore geology of the central SMO. We also thank Luigi Solari and Carlos Ortega for assistance with U-Pb datings and Juan Tomás Vazquez for the elaboration of thin sections.

Appendix A. Supplementary data

Supplementary data to this article can be found online at https://doi.org/10.1016/j.oregeorev.2018.12.020.

References

Abdullin, F., Solari, L., Ortega-Obregón, C., Solé, J., 2018. New fission-track results from the northern Chiapas Massif area, SE Mexico: trying to reconstruct its complex thermo-tectonic history. Rev. Mex. Cienc. Geol. 35 (1), 79–92.

Albinson, T., Norman, D.I., Cole, D., Chomiak, B., 2001. Controls on formation of low

sulfidation epithermal deposits in Mexico: constraints from fluid inclusion and stable isotope data. In: New Mines and Discoveries in Mexico and Central America 8. Society of Economic Geology Special Publication, pp. 1–32.
Ballard, S., 1980. Structural geologic controls at the San Luis mines, Tayoltita, Durango, Mexico (Unpublished M.A. Thesis).
Bonneau, M., 1970. Una nueva área Cretácica fosilífera en el estado de Sinaloa. Bol. Soc. Geol. Mexic. 32, 159–167.
Bryan, S., Ferrari, L., 2013. Large igneous provinces and silicic large igneous provincies: progress in our understanding over the last 25 years. Geol. Soc. Am. Bull. 125, 1053–1078.
Bryan, S.E., Ferrari, L., Reiners, P.W., Allen, C.M., Petrone, C.M., Ramos-Rosique, A., Campbell, I.H., 2008. New Insights into crustal contributions to large-volume rhyolite generation in the mid-Tertiary Sierra Madre Occidental Province, Mexico, revealed by U-Pb geochronology. J. Petrol. 49, 47–77.
Camprubí, A., 2013. Tectonic and Metallogenic History of Mexico. Soc. Econ. Geol. Spec. Publ. 17, 201–243.
Camprubí, A., Albinson, T., 2007. Epithermal deposits in México — update of current knowledge, and an empirical reclassification. Geol. Soc. Am. Spec. Pap. 422, 377–415.
Cassata, W.S., Renne, P.R., 2013. Systematic variations of argon diffusion in feldspars and implications for thermochronometry. Geochim. Cosmochim. Acta 112, 251–287.
Clarke, M., 1986. Hydrothermal geochemistry of Ag-Au veins in the Tayoltita and the San Dimas mining district, Durango and Sinaloa, Mexico (Unpublished Ph.D. dissertation). p. 151.
Clarke, M., Titley, S., 1988. Hydrothermal evolution in the formation of silver-gold veins in the Tayoltita mine, San Dimas district, Mexico. In: New Mines and Mineral Discoveries in Mexico and Central America 8. Society of Economic Geologists Special Publications, pp. 1830–1840.
Campa, M.F., Coney, P.J., 1983. Tectono-stratigraphic terranes and mineral resource distributions in Mexico. Can. J. Earth Sci. 20, 1040–1051.
Damon, P.E., Shafiqullah, M., Clark, K.F., 1981. Evolución de los arcos magmáticos en México y su relación con la metalogénesis. Rev. Mexic. Cienc. Geol. 5, 223–238.
Damon, P., Shafiqullah, M., Clark, K., 1983. Geochronology of the porphyry copper deposits and related mineralization in Mexico. Can. J. Earth Sci. 20, 1052–1071.
Davidson, S., 1932. Geology and ore deposit of Tayoltita, district of San Dimas, Durango, Mexico (Unpublished PhD thesis). p. 172.
Donelick, R.A., O'Sullivan, P.B., Ketcham, R.A., 2005. Apatite fission-track analysis. Rev. Mineral. Geochem. 58 (1), 49–94.
Duque-Trujillo, J., Ferrari, L., Orozco-Esquivel, T., López-Martínez, M., Losndale, P., Bryan, S., Kuesner, J., Piñero-Lajas, D., Solari, L., 2015. Timing of rifting in the southern Gulf of California and its conjugated margins: insight from the plutonic record. Geol. Soc. of Am. Bull. 127, 702–736.
Enriquez, E., Rivera, R., 2001a. Geology of the Santa Rita Ag-Au Deposit, San Dimas District, Durango, Mexico. In: New Mines and Mineral Discoveries in Mexico and Central America 8. Society of Economic Geologists Special Publication, pp. 39–58.
Enríquez, E., Rivera, R., 2001b. Timing of magmatic and hydrothermal activity in the San Dimas District, Durango, Mexico. In: New Mines and Mineral Discoveries in Mexico and Central America 8. Society of Economic Geologist Special Publication, pp. 33–38.
Enriquez, E., Iriondo, A., Camprubí, A., 2018. Geochronology of Mexican mineral deposits. VI: the Tayoltita low-sulfidation epithermal Ag-Au district, Durango and Sinaloa. Bol. Soc. Geol. Mexic. 70, 531–547.
Ferrari, L., Rosas-Elguera, J., 2000. Late Miocene to Quaternary extension at the northern boundary of the Jalisco block, western Mexico: the Tepic-Zacoalco rift revised. Geol. Soc. Am. Spec. Pap. 334, 41–64.
Ferrari, L., López-Martínez, M., Rosas-Elguera, J., 2002. Ignimbrite flareup and deformation in the southern Sierra Madre Occidental, western Mexico-implications for the late subduction history of the Farallon Plate. Tectonics 21, 1035 10.1029/2001TC001302.
Ferrari, L., López-Martínez, M., Orozco-Esquivel, T., Bryan, S.E., Duque-Trujillo, J., Lonsdale, P., Solari, L., 2013. Late Oligocene to Middle Miocene rifting and synextensional magmatism in the southwestern Sierra Madre Occidental, Mexico: the beginning of the Gulf of California rift. Geosphere. https://doi.org/10.1130/GES00925.1.
Ferrari, L., Orozco-Esquivel, T., Bryan, S., Lopez-Martínez, M., Silva Fragoso, A., 2017. Cenozoic extension and magmatism in western Mexico: linking the Sierra Madre Occidental Silicic Large Igneous Province and the Comondú Group with the Gulf of California rift. Earth-Sci. Rev. 183, 115–152.
Ferrari, L., Valencia-Moreno, M., Bryan, S., 2007. Geology of the western Mexican volcanic belt and adjacent Sierra Madre Occidental and Jalisco block. Geol. Soc. Am. Spec. Pap. 334, 65–83.
Folk, R.L., 1974. Petrology of Sedimentary Rocks. Hemphill Publishing Company, Texas.
Gans, P., 1997. Large-magnitude Oligo-Miocene extension in southern Sonora: implications for the tectonic evolution of northwest Mexico. Tectonics 16, 388–408.
Gastil, P., 1975. Plutonic zones in the Peninsular Ranges of southern California and northern Baja California. Geology 3, 361–363.
Goldoff, B., Webster, J.D., Harlov, D.E., 2012. Characterization of fluor-chlorapatites by electron probe microanalysis with a focus on time-dependent intensity variation of halogens. Am. Mineral. 97, 1103–1115.
González León, C.M., McIntosh, W.C., Lozano-Santacruz, R., Valencia-Moreno, M., Amaya-Martínez, R., Rodríguez-Castañeda, J.L., 2000. Cretaceous and Ter- tiary sedimentary, magmatic, and tectonic evolution of north-central Sonora (Arizpe and Bacanuchi quadrangles), northwest Mexico. Geol. Soc. Am. Bull. 112, 600–610.
Hasebe, N., Barbarand, J., Jarvis, K., Carter, A., Hurford, A.J., 2004. Apatite fission-track chronometry using laser ablation ICP-MS. Chem. Geol. 207 (3–4), 135–145.
Henry, C., 1975. PhD Dissertation In: Geology and geochronology of the granitic batholithic complex, Sinaloa, Mexico. University of Texas at Austin, pp. 158.
Henry, C.D., 1986. East-northeast–trending structures in western Mexico: Evidence for oblique convergence in the late Mesozoic. Geology 14 (4), 314.
Henry, C.D., 1989. Late Cenozoic Basin and range structure in western Mexico adjacent to the Gulf of California. Geol. Soc. Am. Bull. 101 (9), 1147–1156.
Henry, D., Fredrikson, G., 1987. Geology of southern Sinaloa adjacent to the Gulf of California. Geol. Soc. Am. Map Chart Ser. 14.
Henry, C.D., Aranda-Gómez, J.J., 2000. Plate interactions control middle-late Miocene proto-Gulf and Basin and Range extension in the southern Basin and Range. Tectonophysics 318, 1–26.
Henry, C., McDowell, F., Silver, L., 2003. Geology and geochronology of granitic batholithic complex, Sinaloa, México: implications for Cordilleran magmatism and tectonics. Geol. Soc. Am. Spec. Pap. 374, 237–273.
Henshaw, P.C., 1953. Geology and Ore Deposit of the San Dimas District, Sinaloa and Durango. Private document. p. 531.
Horner, J., Enriquez, E., 1999. Epithermal precious metal mineralization in a strike-slip corridor: the San Dimas District, Durango, Mexico. Econ. Geol. 94 (8), 1375–1380.
Hurford, A.J., 2019. An historical perspective on fission-track thermochronology. In: Fission-Track Thermochronology and its Application to Geology. Springer, Cham, pp. 3–23.
Le Bas, M.J., Streckeisen, A.L., 1991. The IUGS systematics of igneous rocks. J. Geol. Soc. 148, 825–833.
Le Maitre, R.W., Streckeisen, A., Zanettin, B., Le Bas, M.J., Bonin, B., Bateman, P., et al., 2002. In: Igneous Rocks. A Classification and Glossary of Terms: Recommendation of the International Union of Geological Science, Subcommission on the Systematic of Igneous Rocks, Second ed. Cambridge University Press, pp. 236.
Locke, A., 1918. Unpublished report In: Geologic atlas, San Dimas mining district, Mexico. San Luis Mining Company, Tayoltita, pp. 10.
Love, D.A., Clark, A.H., Hodgson, C.J., Mortensen, J.K., Archibald, D.A., Farrar, E., 1998. The timing of adularia-sericite-type mineralization and alunite-kaolinite-type alteration, Mount Skukum epithermal gold deposit, Yukon Territory, Canada; ^{40}Ar-^{39}Ar and U-Pb geochronology. Econ. Geol. 93, 437–462.
Ludwig, K.R., 2008. Useŕs manual fro Isoplot 3.7. A geochronological toolkit for Microsoft Excel. Berkeley Geochronol. Center Spec. Publ. 4, 77.
McDowell, F.W., Clabaugh, S.E., 1979. Ignimbrites of the Sierra Madre Occidental and their relation to the tectonic history of western Mexico. Geol. S. Am. S. 180, 113–124.
McDowell, F., Keizer, R., 1977. Timing of mid Tertiary volcanism in the Sierra Madre Occidental between Durango City and Mazatlán, Mexico. Geol. Soc. Am. Bull. 88, 1479–1487.
McDowell, F., Roldán-Quintana, J., Amaya-Martínez, R., 1997. Interrelationship of sedimentary and volcanic deposits associated with Tertiary extension in Sonora, Mexico. Geol. Soc. Am. Bull. 109, 1349–1360.
McDowell, F., McIntosh, W., 2012. Timing of intense magmatic episodes in the northern and central Sierra Madre Occidental, western. Geosphere 8, 1505–1526.
McDowell, F., Roldán-Quintana, J., Connelly, J., 2001. Duration of Late Cretaceous-early Tertiary magmatism in east-central Sonora, Mexico. Geol. Soc. Am. Bull. 113, 521–531.
Montoya-Lopera, P., Levresse, G., Ferrari, L., Orozco-Esquivel, T., Hérnandez-Quevedo, G., Mata, L., submitted for publication. New geological, geochronological and geocemical characterization of the telescoped Eocene-Oligocene Ag/Au San dimas epithermal deposit, Mexico. Ore Geol. Rev.
Murray, B.P., Busby, C.J., Ferrari, L., Solari, L.A., 2013. Synvolcanic crustal extension during the mid-Cenozoic ignimbrite flare-up in the northern Sierra Madre Occidental, Mexico: evidence from the Guazapares Mining District region, western Chihuahua. Geosphere 9, 1201–1235.
Nemeth, K.E., 1976. Petrography of the Lower Volcanic Group, Tayoltita-San Dimas District, Durango, Mexico (Unpublished M.A. thesis). p. 141.
Nourse, J., Anderson, T., Silver, L., 1994. Tertiary metamorphic core complexes in Sonora, northwestern Mexico. Tectonics 13, 1161–1182.
Ortega-Gutiérrez, F., Elías-Herrera, M., Morán-Zenteno, D.J., Solari, L., Luna-González, L., Schaaf, P., 2014. A review of batholiths and other plutonic intrusions of Mexico. Gondwana Res. 26 (3–4), 834–868.
Ortega-Obregón, C., Solari, L., Gómez-Tuena, A., Elías-Herrera, M., Ortega-Gutiérrez, F., Macías-Romo, C., 2014. Permian-Carboniferous arc magmatism in southern Mexico: U-Pb dating, trace element and Hf isotopic evidence on zircons of earliest subduction beneath the western margin of Gondwana. Int. J. Earth Sci. 103 (5), 1287–1300.
Paton, C., Hellstrom, J., Paul, B., Woodhead, J., Hergt, J., 2011. Iolite: Freeware for the visualisation and processing of mass spectrometric data. J. Anal. At. Spectrom. 26 (12), 2508–2518.
Petrus, J.A., Kamber, B.S., 2012. VizualAge: A novel approach to laser ablation ICP-MS U-Pb geochronology data reduction. Geostand. Geoanal. Res. 36 (3), 247–270.
Salas, G.P., 1994. Economic geology of Mexico. In: Salas, G.P. (Ed.), Economic Geology, Mexico. Geological Society of America, Geology of North America, P-3, Boulder, Colorado, pp. 1–6.
Servicio Geológico Mexicano, 2002. Carta geológico-minera Borbollones, F13 – A17, escala 1:50,000, estados de Durango y Sinaloa (Technical Report). p. 54.
Smith, D.M., Hall, D.K., 1974. In: Geology of the Tayoltita mine, Durango, Mexico. Society of Mining Engineers of A.I.M.E, pp. 48.
Smith, D., Albinson, T., Sawkins, F., 1982. Geologic and fluid inclusion studies of the Tayoltita silver-gold vein deposit, Durango, Mexico. Soc. Econ. Geol. 1120–1145.
Solari, L.A., Gómez-Tuena, A., Bernal, J.P., Pérez-Arvizu, O., Tanner, M., 2010. U-Pb zircon geochronology by an integrated LA-ICPMS microanalytical workstation: achivements in precision and accuracy. Geostand. Geoanal. Res. 34, 5–18.
Staude, J.M.G., Barton, M.D., 2001. Jurassic to Holocene tectonics, magmatism, and metallogeny of northwestern Mexico. Geol. Soc. Am. Bull. 113 (10), 1357–1374.
Valencia, V., Righter, K., Rosas-Elguera, J., Lopez-Martinez, M., Grove, M., 2013. The age and composition of the pre-Cenozoic basement of the Jalisco Block: implications for

and relation to the Guerrero composite terrane. Contrib. Miner. Petrol. 166 (3), 801–824.
Vermeesch, P., 2009. RadialPlotter: a Java application for fission track, luminescence and other radial plots. Radiat. Meas. v. 44, 409–410.
Vermeesch, P., 2017. Statistics for LA-ICP-MS based fission track dating. Chem. Geol. 456, 19–27.
Vermeesch, P., 2018. IsoplotR: a free and open toolbox for geochronology. Geosci. Front. https://doi.org/10.1016/j.gsf.2018.04.001.
Wiedenbeck, M., Alle, P., Corfu, F., Griffin, W.L., Meier, M., Oberli, F., Spiegel, W., 1995. Three natural zircon standards for U-Th-Pb, Lu-Hf, trace element and REE analyses. Geostand. Newslett. 19 (1), 1–23.
Wilson, F.O., Rocha, S., 1949. Coal deposits of the Santa Clara distric near Tónichy, Sonora, Mexico. U.S. Geol. Surv. Bull. 962A, 80.
Wong, M.S., Gans, P.B., Scheier, J., 2010. The 40Ar/39Ar thermochronology of core complexes and other base- ment rocks in Sonora, Mexico: Implications for Ceno- zoic tectonic evolution of northwestern Mexico. J. Geophys. Res. 115 (B7), B07414.